CONSTRUCTION
INDUSTRY COUNCIL
建造業議會

APPLICATION OF POLYGONAL HIGH STRENGTH CONCRETE-FILLED COMPOSITE COLUMN IN SEISMIC-RESISTANT BUILDINGS IN HONG KONG

RESEARCH SUMMARY

Construction Industry Council
Application of polygonal high strength concrete-filled composite column in seismic-resistant buildings in Hong Kong
Research Summary

Author

Dr Tak-Ming CHAN
The Hong Kong Polytechnic University

Published by

Construction Industry Council,
Hong Kong SAR

DISCLAIMER

The information given in this report is correct and complete to the best of knowledge of the authors and publisher. All recommendations are made without guarantee on the part of the authors or publisher. The authors and publisher disclaim any liability in connection with the use of the information given in this report.

Enquiries

Enquiries on this research may be made to the CIC Secretariat at:

CIC Headquarters
38/F, COS Centre, 56 Tsun Yip Street, Kwun Tong, Kowloon

Tel.: (852) 2100 9000

Fax: (852) 2100 9090

Email: enquiry@cic.hk

Website: www.cic.hk

FOREWORD

Composite structure is an innovative structural form integrating the advantages of concrete and steel, thus it has been widely adopted worldwide. Design guidelines have been well established for steel elements with regular sections, e.g. circular steel tube. However, there is still a knowledge gap for polygonal concrete-filled composite element while it provides some merits over the traditional composite element with circular steel tube. One merit is that polygonal section is easier to fabricate than large-diameter circular section and polygonal section is also easier to connect with other sections.

When the industry evolves into Design for Manufacture and Assembly (DfMA), composite elements with polygonal section are deemed to become more and more popular. The Construction Industry Council (CIC) well recognized the needs of the industry and supported this innovative project proposed by the Hong Kong Polytechnic University.

Led by Dr Tak-Ming Chan, the research team conducted a large amount of work in experimental tests and finite element analysis to produce this solid, well presented and comprehensive research report. I would like to congratulate and give thanks to Dr Chan and all those who contributed to the research project.

Ir Albert CHENG
Executive Director
Construction Industry Council

PREFACE

Concrete-filled steel tubular members have been increasingly used worldwide because of the favourable composite structural behaviour and corresponding shorter construction time. In modern society, the application of high strength materials is of vital importance, in particularly for high-rise buildings, as it can reduce the dimensions of structural members resulting in larger usage floor area, fewer material consumptions, lighter structural self-weight, lower constructional expenses as well as lower carbon footprints.

In terms of structural performance, circular tubes and elliptical tubes can effectively confine the in-filled concrete. However, in Hong Kong, typical off-the shelf hollow sections are insufficient for the application in the high-rise buildings. Depending on the construction requirements, this research project proposed the use of polygonal shaped tubes to mimic circular and elliptical counterparts. This research project was sponsored by the CIC to develop the design recommendations for the polygonal high strength concrete-filled tubular columns.

Upon completion of the project, a series of design recommendations in line with the Eurocode 4 regarding the octagonal hollow and concrete-filled steel tubular columns have been proposed based on the experimental and analytical results from this project. It was also found that the current design rules prescribed in Eurocode 4 are applicable to the design of octagonal high strength concrete-filled tubular beams and beam-columns. It was observed from the cyclic tests that polygonal high strength concrete-filled tubular columns have outstanding energy dissipation capacity. Therefore, polygonal high strength concrete-filled tubular column could be an alternative column form in the construction of high-rise buildings.

Dr Tak-Ming CHAN
Department of Civil and Environmental Engineering
The Hong Kong Polytechnic University

RESEARCH HIGHLIGHTS

Advances in construction research and innovation are driving forces that impact the HK economy by enhancing competitiveness and effectiveness. Adopting new structural form has a crucial role to play. Thus, developing and applying the new structural system – polygonal high strength concrete-filled composite column (CFCC) – is the focus of this project. This system involves in-filling high strength concrete inside a pre-fabricated polygonal steel tube to form a composite member. The application of traditional CFCC has shown to offer fast-track construction, as it eliminates the need of temporary formwork for concrete-casting as well as promoting the use of pre-fabricated connection units which can be shop-welded on the outer skin of the steel tube. This minimises the on-site labour welding activities. This system has also shown to improve strength, stiffness and ductility by comparing to their reinforced concrete or bare steel counterparts. It is attributed to the fact that the outer steel tube prevents or delays lateral expansion and failure of the concrete core, which in turn mitigates inward buckling of the steel hollow section. This enhanced strength and stiffness encourage the use of columns with smaller sections, which improves the usable floor area as well as the working space for workers during construction. On top of the above structural efficiency, the composite action of the CFCC has also been proved to have favourable energy dissipative performance. Hence CFCC has been used in seismic-resistant buildings world-wide. Hong Kong has been leading the world in using high strength concrete in high-rise buildings. The current HK code of practice (CoP) on the structural use of concrete (2013) covers concrete grade up to C100 (corresponding to characteristic compressive cube strength of 100 MPa) complementing the design specifications for the current Eurocode 2 – Design of concrete structures (2004). Two distinctive features are noted for high strength concrete. (i) High stiffness: the initial stiffness of grade C100 concrete can be 50% higher than that for grade C40 concrete, which is substantial for high-rise buildings design in which deflection is normally the governing factor. (ii) Brittle failure: the sharp decline in the post-peak response leads to undesirable brittle failure. To utilise its performance, the second feature can be eliminated by confining the high strength concrete by outer steel tubes. Circular steel tube is the best option as it provides uniform pressure to confine the concrete. However, it is challenging to fabricate large diameter circular steel tube for high-rise building applications in Hong Kong. Thus, this project proposes the use of polygonal shaped tubes fabricated from flat plates to mimic the circular counterparts.

Currently, there are no design guidelines in implementing this polygonal high strength CFCC in Hong Kong and worldwide. For composite design, the HK CoP for the Structural Use of Steel (2011) and the Eurocode 4 – Design of Composite Steel and Concrete Structures (2004) cover normal strength composite steel-concrete columns with concrete grade up to C60 only. Current Eurocode 8 – Design of Structures for Earthquake Resistance in Composite Steel-Concrete Building also targets concrete grade up to C40. Thus, this research carried out a series of tests to bridge the knowledge gaps. Prior to the main tests, to obtain the material properties, total 26 steel tensile coupon tests and 64 concrete material tests were carried out. To address the cross-section classification of octagonal hollow sections and to assess the confinement effect of octagonal concrete-filled steel tubular columns, 38 stub column tests including eight hollow specimens, nine plain concrete specimens and twenty-one concrete-filled specimens under monotonic compression were conducted with the aid of the in-house 450 tons MTS compression machine and the 300 tons/1000 tons (tension/compression) servo-controlled multipurpose testing machine at The Hong Kong Polytechnic University. To investigate the flexural behaviour and energy dissipative performance of octagonal hollow and concrete-filled sections, 17 beam and beam-column tests were performed under monotonic or cyclic loading with the aid of the in-house 300 tons/1000 tons (tension/compression) servo-controlled multipurpose testing machine as well as the tailored testing system at The University of Hong Kong.

Based on the experimental observations and theoretical analyses, design recommendations on (1) the design of octagonal concrete-filled sections under axial compression, bending, and combined bending and axial compression and (2) hysteretic model under cyclic load for seismic application, were proposed. The design recommendations have been assessed against the test results. The comparisons with a good agreement between design recommendations and the test results indicate design recommendations could predict the behaviours of octagonal concrete-filled members with acceptable effectiveness and conservatism.

CONTENTS

1 INTRODUCTION

1.1 Background

The advancement of construction research and innovation contributes to the economic strength of Hong Kong and promote the quality of life of the general public with a safe and efficiently-built environment. Hong Kong construction industry is renowned for her efficiency and high productivity. To strengthen this position, this project proposes an innovative composite steel-concrete structural form which will enhance productivity in the construction sector, and also promotes the use of Eurocodes for composite steel-concrete construction, EN 1994-1-1 (CEN, 2004), and seismic design, EN 1998-1 (CEN, 2004) in Hong Kong (Legislative Council, 2014).

Composite steel-concrete construction system has favourable advantages over the traditional systems. It combines the structural and construction efficiency from both the reinforced-concrete and steel construction. In particular, it promotes faster construction cycle by minimising on-site labour activities as it encourages the use of pre-fabricated units and also reduces the amount of formworks. The optimised structural performance on strength and stiffness from the composite action reduces structural member size which leads to improved working and usable floor space as well as reduced foundation size. This will further minimise on-site ground work activities. The concrete component can also provide the required fire resistance. Another crucial beneficial structural performance is the enhanced energy dissipation capabilities which are essential for seismic design.

One of the key components in a composite system is the concrete-filled steel tubular members (CFSTs). This structural arrangement allows casting concrete into the steel hollow section without any use of temporary formworks which reduces cost and time. Figure 1 shows some typical CFSTs which includes rectangular, circular and elliptical hollow sections (Chan *et al.*, 2010).

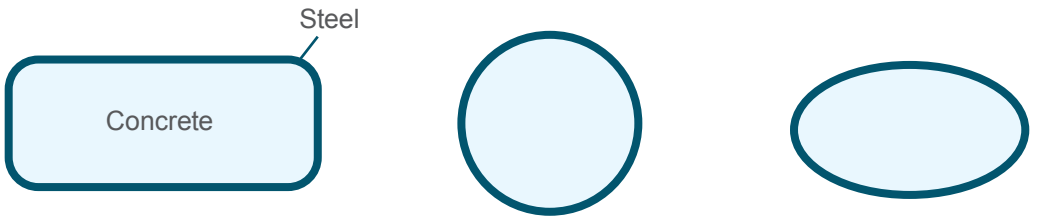

Rectangular hollow section (RHS) | Circular hollow section (CHS) | Elliptical hollow section (EHS)

Figure 1 Typical concrete-filled steel tubular columns

In this structural arrangement, the outer steel tube can serve as a permanent formwork for the in-filled concrete whilst due to its own strength and stiffness, it can also provide temporary support to other construction activities throughout the construction cycle. This reduces on-site labour activities and promotes efficient construction technique. In terms of structural performance, the steel tube mainly from those with constant (CHS) or varying curvature (EHS) can confine the in-filled concrete. It delays the lateral expansion and failure of the concrete core which in turn mitigates inward buckling of the steel tube. This enhances strength, stiffness, ductility and energy dissipative performance of the concrete-filled composite column. Previous results from Sheehan and Chan (2014), as shown in Figure 2, indicate that the energy dissipation performance of concrete-filled CHS are superior to their hollow counterparts, and the concrete-filled CHS can sustain larger number of cyclic load to fracture. The CFST structural arrangement also promotes the use of pre-fabrication. Figure 3 shows a typical pre-fabricated steel unit in which a channel (with pre-drilled holes) is shop-welded to the steel rectangular hollow section column. This steel prefabricated unit will then be shipped to the construction site and on-site bolted to the flooring system through the angles as shown in the figure. This minimises on-site welding works and promotes higher quality control.

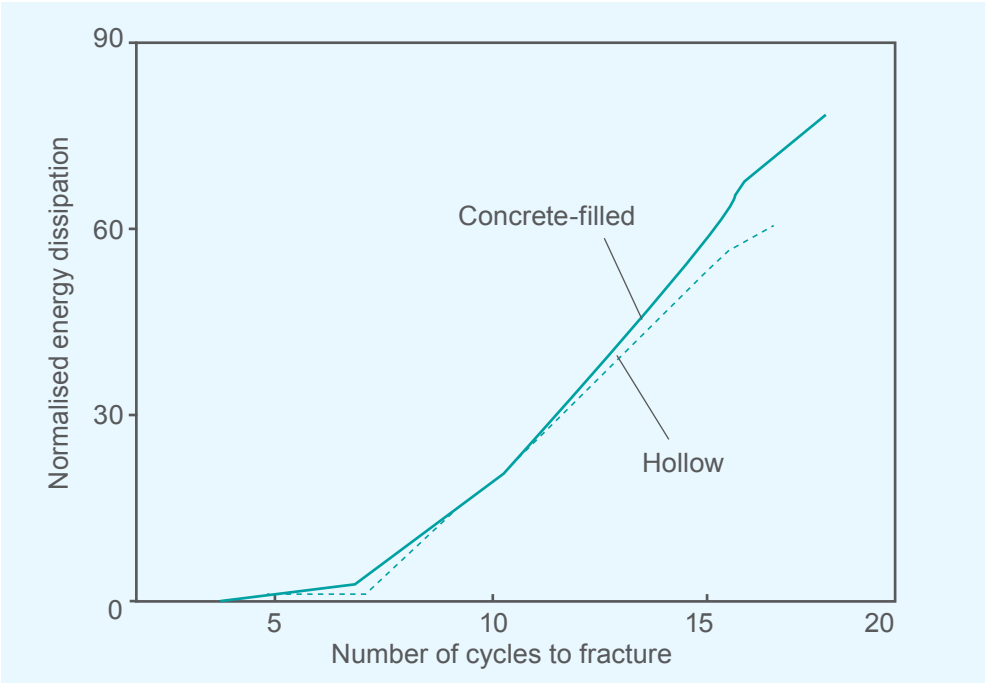

Figure 2 Accumulated energy dissipation for hollow and concrete-filled CHS.

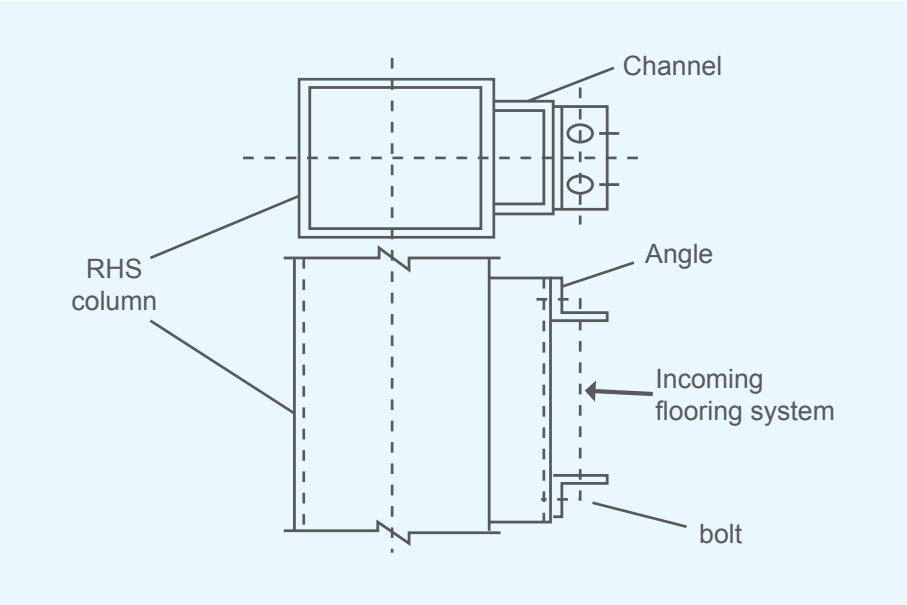

Figure 3 Pre-fabricated connection

In Hong Kong, typical off-the shelf hollow sections (e.g. up to 500 mm in diameter for CHS) are insufficient for the application in high-rise buildings. In addition, it is challenging to fabricate large diameter (e.g. 2000 mm) circular steel tube of thickness (e.g. 40 mm). Therefore, this project proposes the use of prefabricated polygonal shaped tubes to mimic the tubular counterpart. Figure 4 displays some examples of polygonal shaped columns which are fabricated by welding the flat steel plates. Depending on the construction requirements, hexagonal and octagonal shaped can be fabricated to mimic the EHS and CHS counterparts. Due to the pronounced confinement effect, this project focuses on the octagonal shape.

Hong Kong has been leading the world in using high strength concrete in high rise buildings. To exploit this local construction experience, this project will target the high strength (HS) concrete with a characteristic compressive cube strength up to 100 MPa. Comparing to normal strength concrete, HS concrete shows higher initial stiffness and marked brittle failure as displayed in Figure 5. The former property is beneficial as stiffness is an important parameter for high-rise building design while the latter property may limit their application in seismic situation. Thus, to eliminate the deficiency over brittle failure, this project proposes to confine the high strength concrete with a fabricated octagonal shaped column.

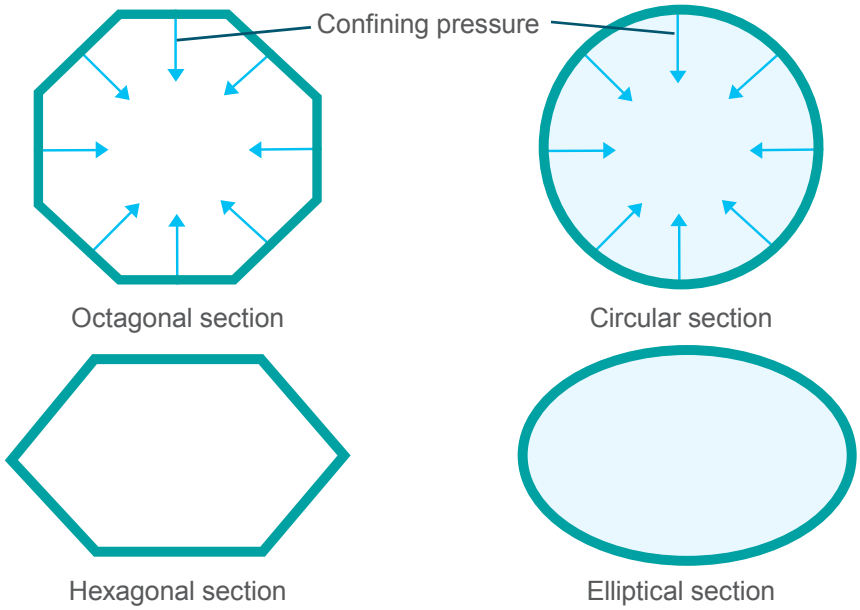

Figure 4 Fabricated polygonal shaped columns

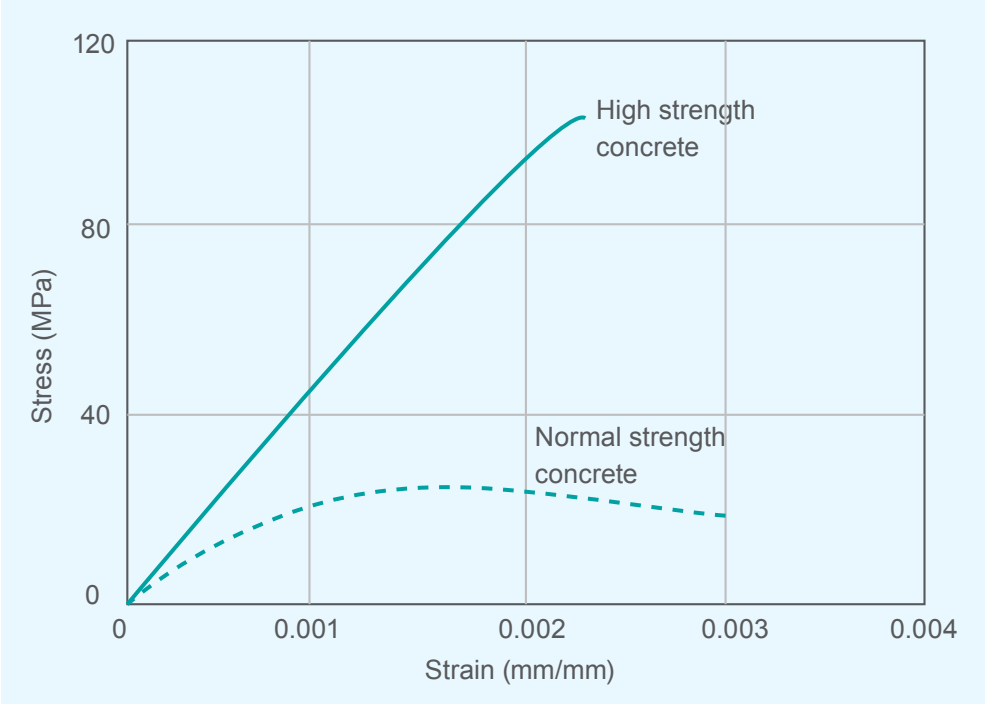

Figure 5 Typical stress-strain curves for normal and high strength concrete

1.2 Aims and Objectives

Currently, there are no design guidelines in implementing this polygonal high strength CFSTs in Hong Kong and worldwide. The current Hong Kong Code of Practice on the Structural Use of Concrete (CoP Concrete, 2013) covers concrete grade up to C100 (corresponding to characteristic compressive cube strength of 100 MPa) complementing the design specifications for the current Eurocode 2 (EN 1992-1-1) – Design of Concrete Structures (CEN, 2004). However, for composite steel-concrete design, the Hong Kong Code of Practice for the Structural Use of Steel (CoP Steel, 2011) and the Eurocode 4 (EN 1994-1-1) – Design of Composite Steel and Concrete Structures covers normal strength composite steel-concrete columns up to concrete grade of C60 only. Current Eurocode 8 (EN 1998-1) – Design of Structures for Earthquake Resistance in Composite Steel-concrete Building also targets concrete grade up to C40.

Therefore, the overall aims of the project are:

(1) To investigate the confinement performance on polygonal high strength (HS, up to concrete grade of C100) concrete-filled steel tubular columns under monotonic load;

(2) To investigate the energy dissipative performance on polygonal CFST beam-columns under cyclic load for seismic application;

(3) To develop statistically validated design rules on confinement and energy dissipation readily available for use in construction industry;

(4) To promote the use of EN 1994-1-1 on composite steel-concrete construction and EN 1998-1 on seismic design in Hong Kong.

And the individual measurable objectives are:

(1) To experimentally examine the confinement effect on the high strength concrete by the polygonal shaped tube under monotonic load;

(2) To experimentally examine the energy dissipation performance of the CFSTs under cyclic load;

(3) To derive statistically validated design rules, written in line with Eurocode terminology, on confinement model;

(4) To derive statistically validated design model, written in line with Eurocode terminology, on energy dissipation;

(5) To disseminate the results in the form of technical structural design guidance and through presentations in technical seminars and conferences in Hong Kong.

1.3 Scope

In this project, the laboratory tests have been carried out at The Hong Kong Polytechnic University and The University of Hong Kong, exploiting the existing expertise and facilities, which will be described in detail in the next chapter.

2 RESEARCH METHODOLOGY

In this project, the laboratory tests (Work Package 1) were firstly carried out at The Hong Kong Polytechnic University and The University of Hong Kong, exploiting the existing expertise and facilities. And this was complemented by the development of practical design guidance (Work Package 2).

2.1 Work Package 1 (WP1) – Physical Testing

To develop statistically validated design rules, a comprehensive set of experimental evidences are crucially required to justify and validate the design models. A thorough experimental investigation was carried out in this project to investigate the performance of the octagonal shaped high strength composite column fabricated from flat steel plates. Three concrete grades of C30, C60 and C100 were examined to bridge the knowledge gap between the HK CoP Steel and CoP Concrete as well as to assess the current provisions in EN 1994-1-1 and EN 1998-1. The nominal steel grade of S355 based on the HK Steel code for the flat plates was used. The local plate width to thickness ratio was designed accordingly. Fundamental material tests were firstly carried out on the parent steel and concrete materials. Material tests were also conducted on the fabricated steel section to examine the effect of cold-forming process and welding. To obtain the material properties, in total, 26 steel tensile coupon tests and 64 concrete material tests were carried out.

To address the cross-section classification of octagonal hollow sections and to assess the confinement effect, 38 stub column tests including eight hollow specimens, nine plain concrete specimens and twenty-one concrete-filled specimens under monotonic compression were conducted with the aid of the in-house 450 tons MTS compression machine and the 300 tons/1000 tons (tension/compression) servo-controlled multipurpose testing machine at The Hong Kong Polytechnic University. To investigate the energy dissipative performance, 17 beam and beam-column tests were performed under monotonic or cyclic loading with the aid of the in-house 300 tons/1000 tons (tension/compression) servo-controlled multipurpose testing machine as well as the tailored testing system at The University of Hong Kong. Prior to the tests, geometric information, material properties, residual stresses due to welding and local initial geometric imperfections were measured.

Material Testing

To obtain the material properties of steel and concrete, in total, 26 steel tensile coupon tests were carried out using an in-house Instron 8800 Fatigue Testing System with a capacity of 500 kN at The Hong Kong Polytechnic University as shown in Figure 6 and 64 concrete material tests were carried out with the aid of an in-house ServoPlus concrete testing machine with a capacity of 3000 kN as shown in Figure 7.

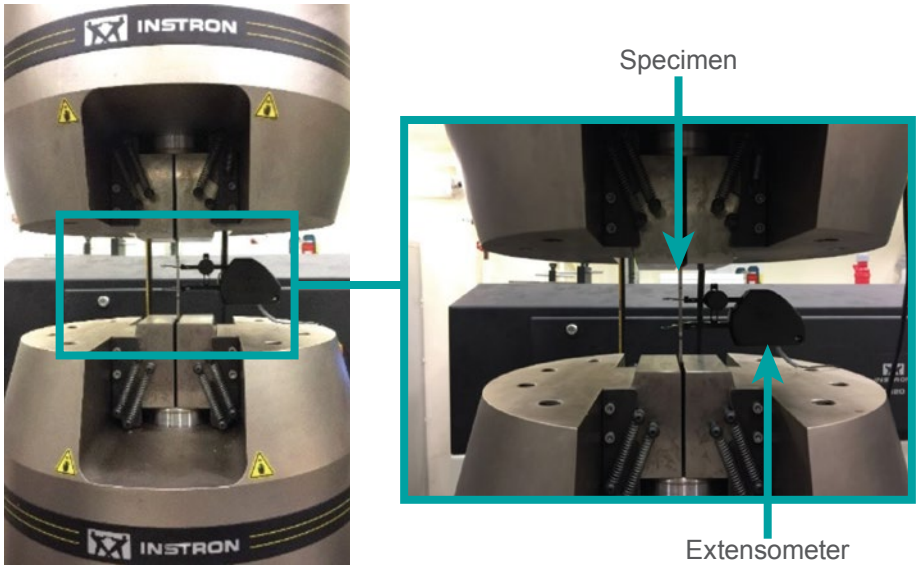

Figure 6 Steel tensile coupon tests.

Figure 7 Concrete material tests.

Axial Compression Behaviour of Hollow Steel Stub Columns

An experimental study on the axial compression behaviour of hollow steel stub columns was carried out using an in-house 450 tons MTS compression machine and the 300 tons/1000 tons (tension/compression) servo-controlled multipurpose testing machine at The Hong Kong Polytechnic University. The test programme included eight stub steel tubes with three different cross-section shapes, namely circular, rectangular and octagonal cross-sectional shapes. Figure 8 presents the test setup for the stub column tests of hollow sections. The experimental results with regard to ultimate capacities were presented and discussed.

Axial Compression Behaviour of CFST Stub Columns

An experimental investigation on the axial compression behaviour of concretefilled steel tubes was conducted with the aid of an in-house 300 tons/1000 tons (tension/compression) servo-controlled multipurpose testing machine at The Hong Kong Polytechnic University. In total, twenty-one CFST stub columns with circular, rectangular and octagonal cross-sections were tested. Three concrete grades with compressive cylinder strengths around 38 MPa, 80 MPa and 112 MPa, were used to infill the hollow steel tubes to form the composite sections. The test setup for the composite stub column tests is depicted in Figure 9. The experimental results with regard to ultimate capacities and confinement effect were presented and discussed.

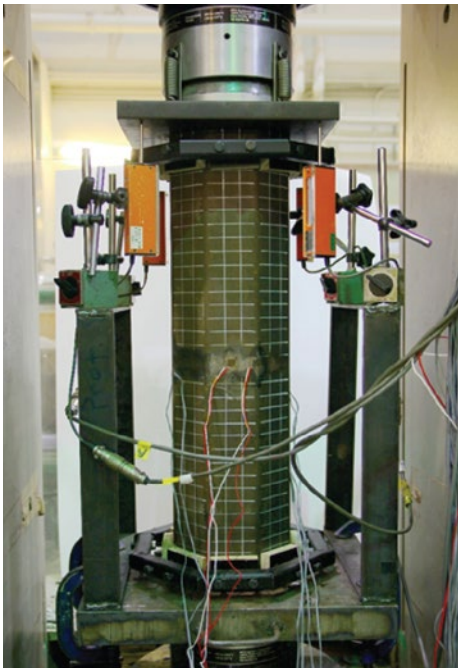

Figure 8 Hollow tube stub column test setup

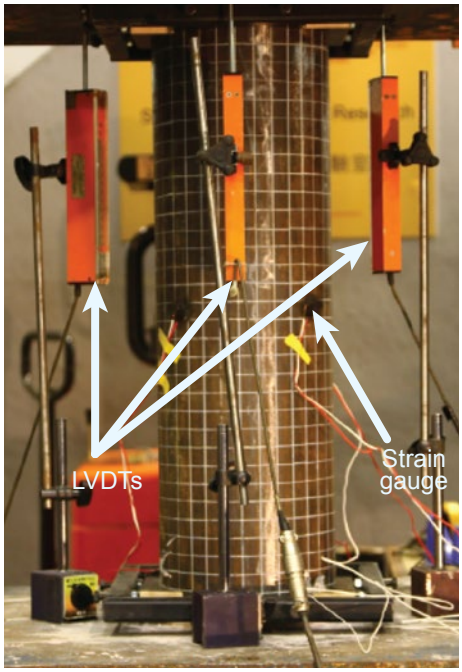

Figure 9 CFST stub column test setup

Octagonal CFST Beams

An experimental study on the flexural behaviour of octagonal CFST beams was conducted with the aid of an in-house testing frame at The Hong Kong Polytechnic University. Details of test setup are presented in Figure 10. A total of eight octagonal CFST beams were tested under monotonic or cyclic lateral load without axial load. Three concrete grades with the target concrete cylinder strengths ranging from 30 MPa to 90 MPa were used to infill the specimens to examine the effect of concrete grades. And two hollow counterparts were tested as well to investigate the effect of concrete infilling. The experimental results with regard to ultimate strengths, initial flexural stiffness and cumulative dissipated energy were discussed.

Cyclic Behaviour of Octagonal CFST Beam-columns

An experimental study on the flexural behaviour of octagonal CFST beam-columns was carried out with the aid of a testing frame at The University of Hong Kong, as shown in Figure 11. A total of nine octagonal CFST beam-columns with different parameters, including the axial load level and the concrete cylinder strength, were tested under cyclical lateral load with or without constant axial load. The axial load level varies from 0 to 0.5, while the concrete cylinder strength ranges from 30 MPa to 90 MPa. The experimental results with regard to ultimate strengths, displacement ductility, initial flexural stiffness and cumulative dissipated energy were presented and discussed.

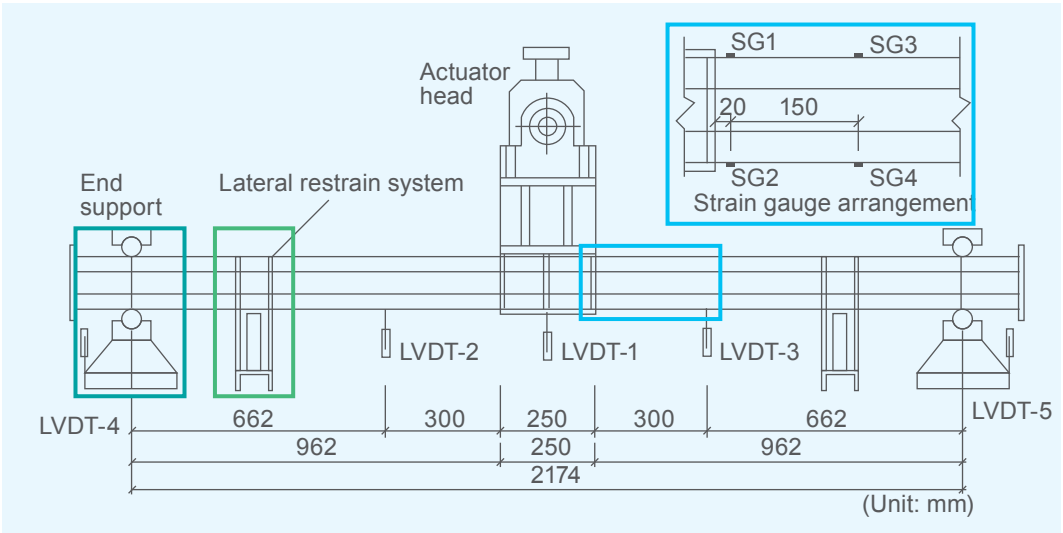

(a) Schematic view of beam tests

Figure 10 Schematic and experimental views of the test setup

(b) Experimental view of beam tests

(c) Lateral restrain system

(d) End support

Figure 10 Schematic and experimental views of the test setup

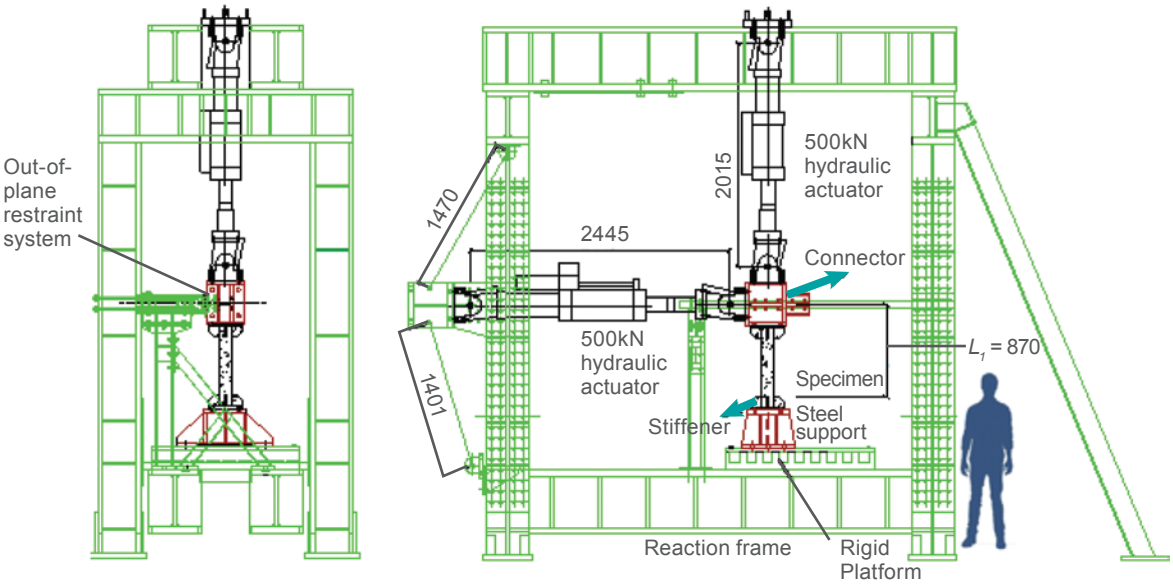

(a) Schematic side view

(b) Schematic front view

(c) Lateral view of the experiment

(d) Front view of the experiment

Figure 11 Schematic and experimental views of the test setup (Unit: mm)

2.2 Work Package 2 (WP2) – Development of Design Guidance

It is the development of design rules that has the most immediate impact on practice. Currently, there is no guidance for the design of polygonal high strength concrete-filled composite column in Hong Kong and worldwide. In this project, it has developed the following key design rules, thereby enabling an informed choice for their use in composite steel-concrete construction in Hong Kong: (1) design rules on compressive resistance on polygonal high strength CFCC under monotonic load with due considerations of the confinement effect and (2) hysteretic model under cyclic load for seismic application. That could facilitate the use of this structural form both in Hong Kong and other regions.

Axial Compression Behaviour of Hollow Steel Stub Columns

Cross-section slenderness limit to distinguish Class 1-3 and Class 4 was proposed based on the test results in this project together with existing test database.

Axial Compression Behaviour of CFST Stub Columns

Design equations to predict the cross-section axial compression capacity in line with Eurocode terminology was proposed based on the test results in this project together with existing test database. The confinement effect of octagonal CFST sections was considered in the design equations.

Octagonal CFST Beams and Beam-columns

The axial compression and bending interaction curve specified in EN 1994-1-1 was used to assess the efficiency of EN 1994-1-1 in the design of octagonal CFST beams and beam-columns.

Analytical Hysteretic Model

An analytical hysteretic model to predict the cyclic behaviour of octagonal CFST beams and beam-columns was proposed based on the test observations.

3 RESEARCH FINDINGS AND DISCUSSION

This report has presented a combined experimental and theoretical investigation on the structural behaviours of CFSTs with polygonal cross-sections. The polygonal steel tubes provide confinement to the infilled concrete, and the concrete in turn could suppress the local buckling of the steel tubes when subjected to uniaxial compression or the combined axial load and lateral loading.

A large number of experimental tests have been presented in this report, including monotonic axial compression tests on hollow steel stub columns with circular, square and octagonal cross-sections, monotonic axial compression tests on CFSTs with circular, square and octagonal cross-sections, and cyclic tests on octagonal CFST beams and beam-columns. Apart from the experimental investigations, theoretical analysis of the behaviour of polygonal CFSTs has also been presented. The cross-section slenderness limit for octagonal hollow sections and design equations for axial load capacity of octagonal CFSTs in line with the Eurocode terminology were proposed. In addition, a hysteretic model for CFST beam-columns under combined axial compression and lateral load was also developed.

3.1 Axial Compression Behaviour of Hollow Steel Stub Columns

Eight tubular steel stub columns with cross-section shapes of octagonal, circular and square were tested under monotonic axial compression test. The test results are summarized in Table 1, in which N_u is the maximum test axial load of the specimens; $f_{0.2,sc}$ is the 0.2% proof stress for the stub hollow steel tubes; $f_{u,sc}$ is the ultimate stress for the stub hollow steel tubes; $N_{0.2,f}$ is the yield load capacity calculated from the 0.2% proof stress of the flat coupon while $N_{0.2,t}$ is the yield load capacity calculated from $f_{0.2,t,}$ the averaged 0.2% proof stress from the tensile coupons weighted by the cross-sectional area of flat and corner region.

$$f_{0.2,t} = \left(\frac{\sum A_{corner} f_{0.2,corner} + \sum A_{flat} f_{0.2,flat}}{A} \right) \quad (1)$$

where A_{corner} and A_{flat} are the cross-sectional area of the corner regions and the flat regions, $f_{0.2,corner}$ and $f_{0.2,flat}$ are the 0.2% proof stress from the tensile coupon test of corner coupons and flat coupons and A is the total area of the cross-section. For CHS, $f_{0.2,t}$ is directly obtained from the test results of curved coupon. The octagonal specimen was labelled as OctHS while CHS and SHS stand for circular and square specimens respectively. The normalized axial stress-axial strain relationships of all hollow specimens and corresponding failure modes are shown in Figure12 and Figure 13.

Table 1: Test results of stub column tests

Stub column	N_u (kN)	$f_{0.2,sc}$(MPa)	$f_{u,sc}$(MPa)	$N_u/N_{0.2,f}$	$N_u/N_{0.2,t}$
OctHS-1	1466	405	471	1.23	1.14
OctHS-2	1441	397	466	1.22	1.13
OctHS-3	1451	399	467	1.22	1.13
CHS-1	1830	489	504	--	1.11
CHS-2	1770	485	500	--	1.11
CHS-3	1760	478	501	--	1.11
SHS-1	2210	--	470	0.99	0.97
SHS-2	2161	--	469	0.99	0.97

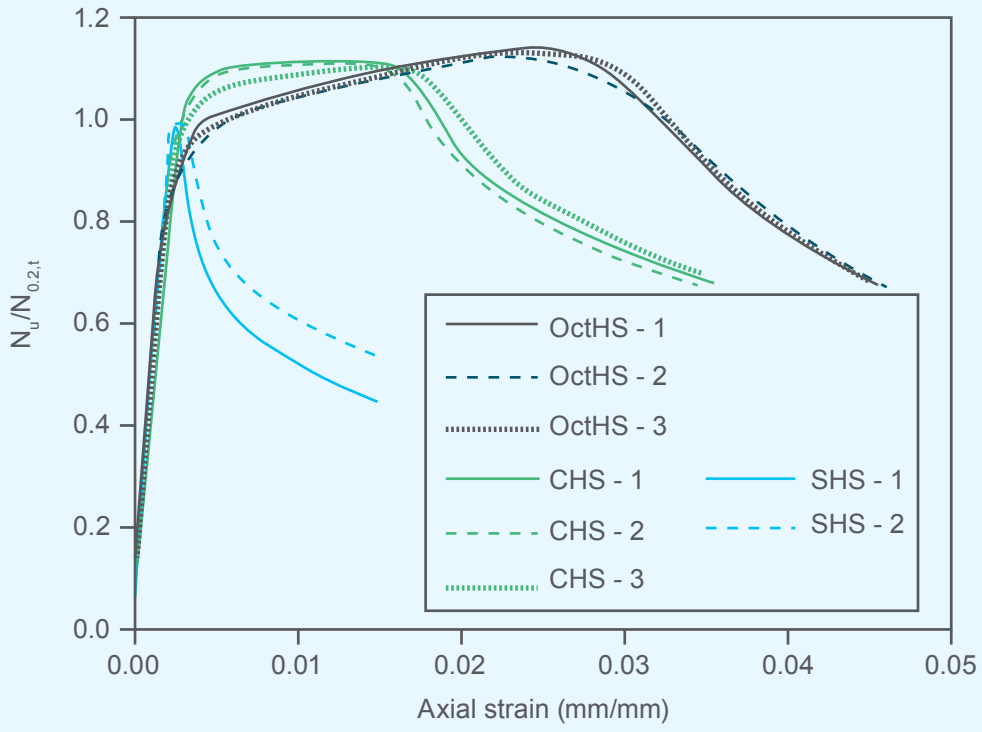

Figure 12 Normalized stress-strain relationship of hollow specimens

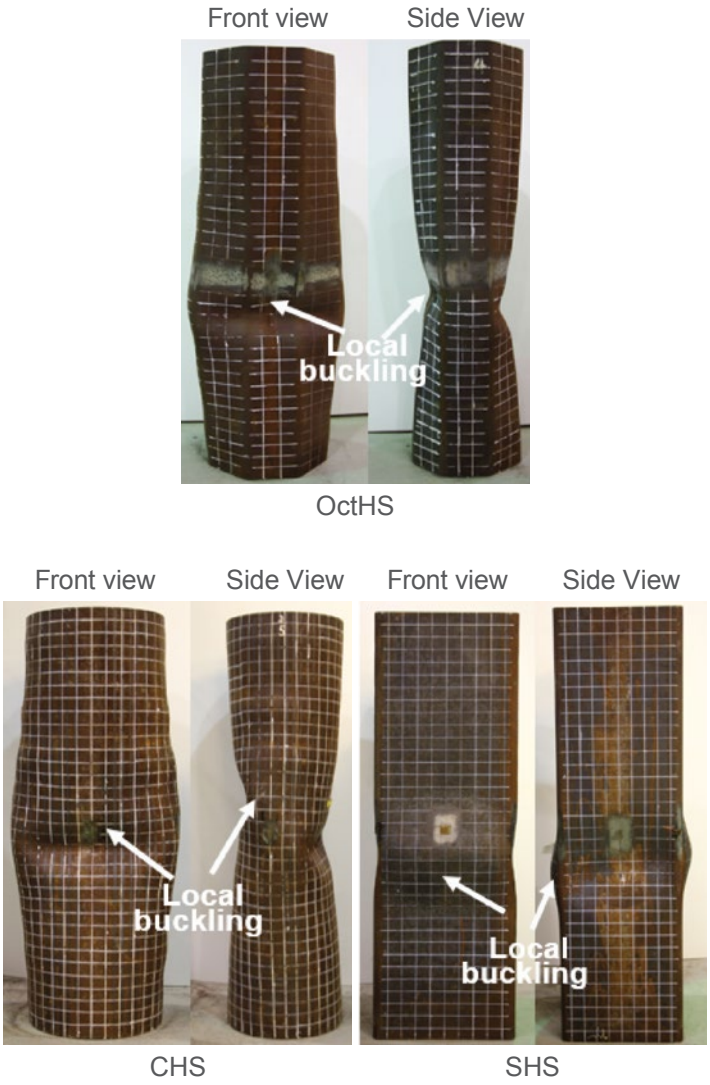

Figure 13 Failure modes of the specimens

Finite element analysis (FEA) was conducted with the aid of the commercial finite element software package ABAQUS (2013). The developed FEA was validated against the test results, as shown in Figure 14. The test results were replicated accurately in both load capacity and load-end shortening response by the FE model.

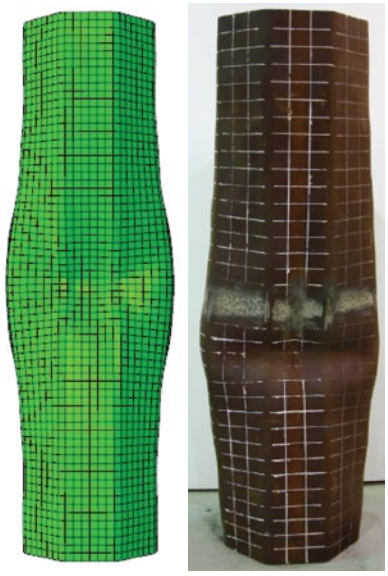

OctHS

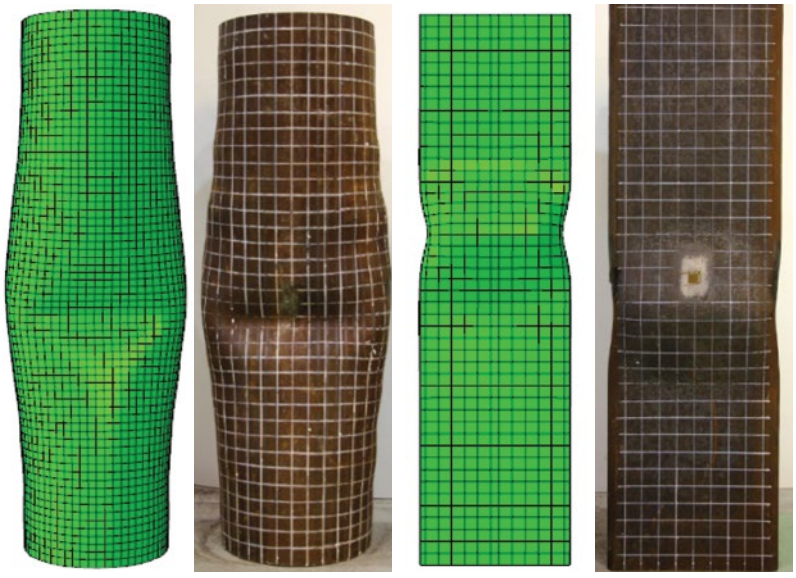

CHS SHS

Figure 14 FE prediction of failure modes

In hollow section stub column tests, it was observed that the stocky octagonal cross-section shows a very similar cross-sectional capability in compression comparing with circular cross-section, and has a better performance compared to square cross-section with a same equivalent width. The current design provision, EN 1993-1-1 and in ASCE standard ASCE/SEI 48-11 (2011), cannot provide a satisfactory cross-section classification on cross-section slenderness for plate buckling (*b/t*) for octagonal hollow section, where b is the width of flat side excluding the corner regions and t is the thickness of the tube. A tightened slenderness limit was proposed in Eq. 2 based on the test results and FEA results, as shown in Figure 15. N_y is the load capacity of the steel section calculated from the yield stress of the material.

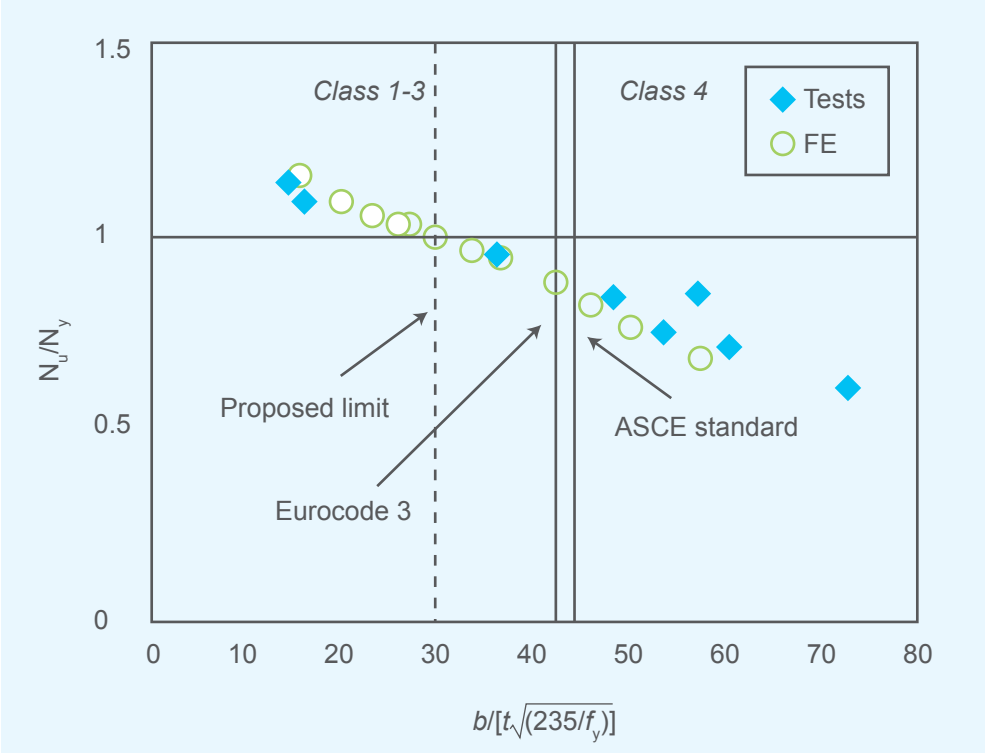

Figure 15 N_u/N_y versus $b/[t\sqrt{(235/f_y)}]$ for octagonal cross-section

$$b / t \leq 29.8\sqrt{(235 / f_y)} \quad (2)$$

An alternative way for the section classification of octagonal cross-section uses the slenderness parameter in circular cross-section which is related to *D/t* ratio. The equivalent circle with the same perimeter of the octagonal cross-section measured at the mid-thickness level, D_p, is suggested as the equivalent diameter with a circular section shares the same cross-sectional area with the original octagonal cross-section. It is concluded that an equivalent circle approach could be adopted for the section classification of octagonal cross-sections based on EN1993-1-1, as shown in Figure 16.

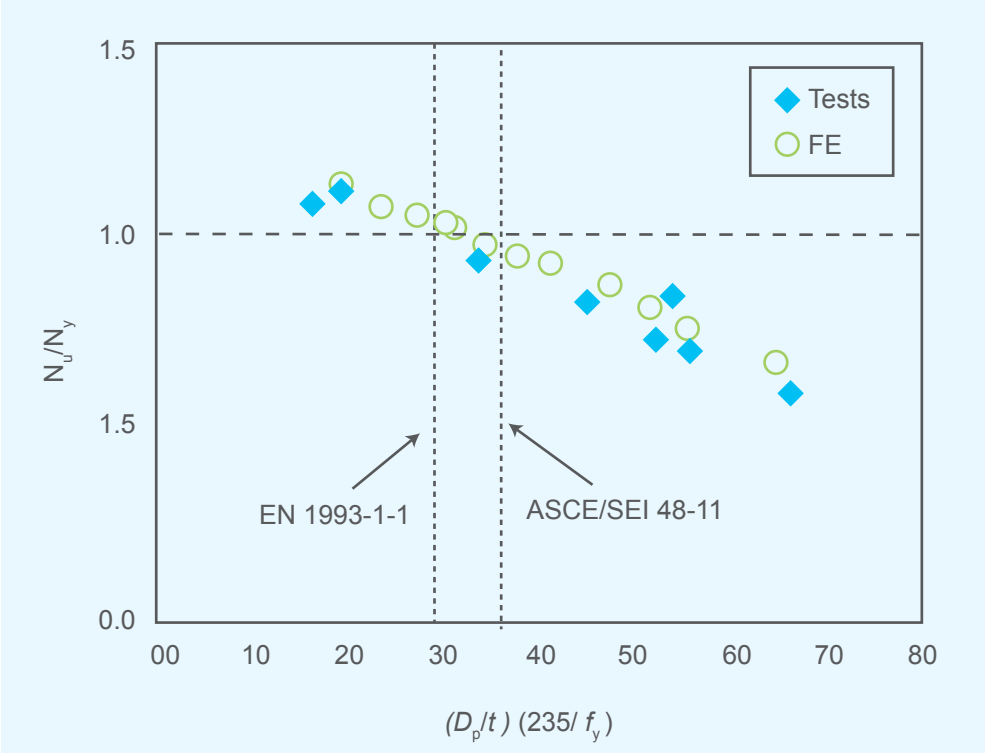

Figure 16 N_u/N_y versus $D/[t(235/f_y)]$ for octagonal cross-section

3.2 Axial Compression Behaviour of CFST Stub Columns

Twenty-one CFST stub columns with cross-section shapes of octagonal, circular and square were tested under monotonic axial compression test. The test results are summarized in Table 2, in which f_y is steel yield strength, f_c' is concrete compressive cylinder strength, ξ is the confinement ratio used to indicate the level of confinement, N_u is the maximum test axial load of the specimens. The normalized axial load-end shortening curves of all CFST specimens and failure modes of typical specimens are shown in Figure 17 and Figure 18.

Table 2 Results of stub column tests

Specimens	f_y (MPa)	f_c' (MPa)	ξ	N_u (kN)
30C-1	451	38	1.54	3503
30C-2	451	38	1.54	3519
30O-1	413	38	1.52	2733
30O-2	413	38	1.52	2680
30S-1	485	38	1.68	3488
30S-2	485	38	1.68	3452
50C-1	453	80.5	0.73	4463
50C-2	453	80.5	0.73	4423
50O-1	413	80.5	0.71	3543
50O-2	413	80.5	0.71	3549
50S-1	485	80.5	0.79	4921
50S-2	485	80.5	0.79	4973
80C-1	453	112.1	0.53	5071
80C-2	453	112.1	0.53	5040
80C-3	453	112.1	0.53	5099
80O-1	413	112.1	0.51	4199
80O-2	413	112.1	0.51	4153
80O-3	413	112.1	0.51	4203
80S-1	485	112.1	0.57	6060
80S-2	485	112.1	0.57	6298
80S-3	485	112.1	0.57	6218

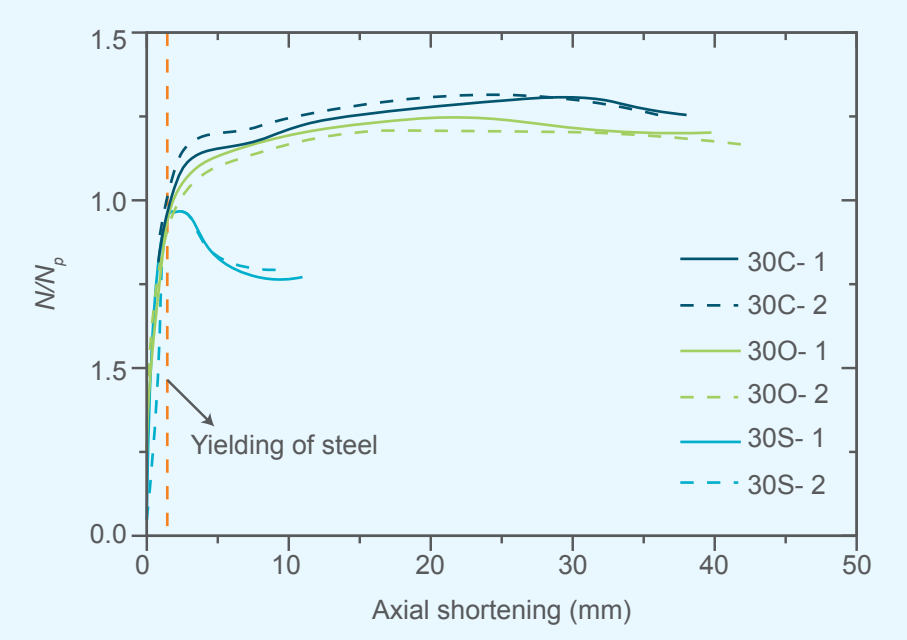

(a) C25/30

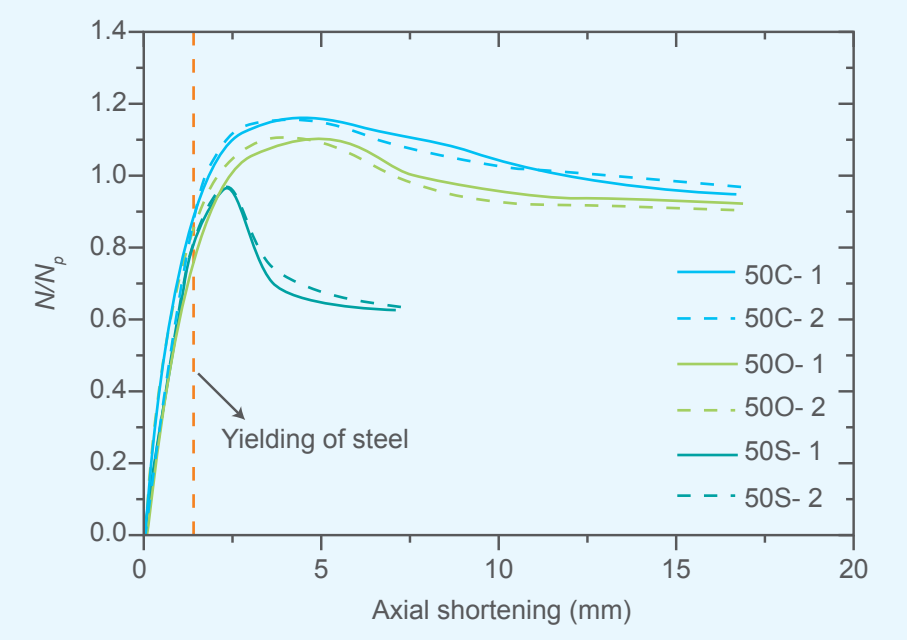

(b) C50/60

Figure 17 Normalized axial load-end shortening curves of CFST specimens

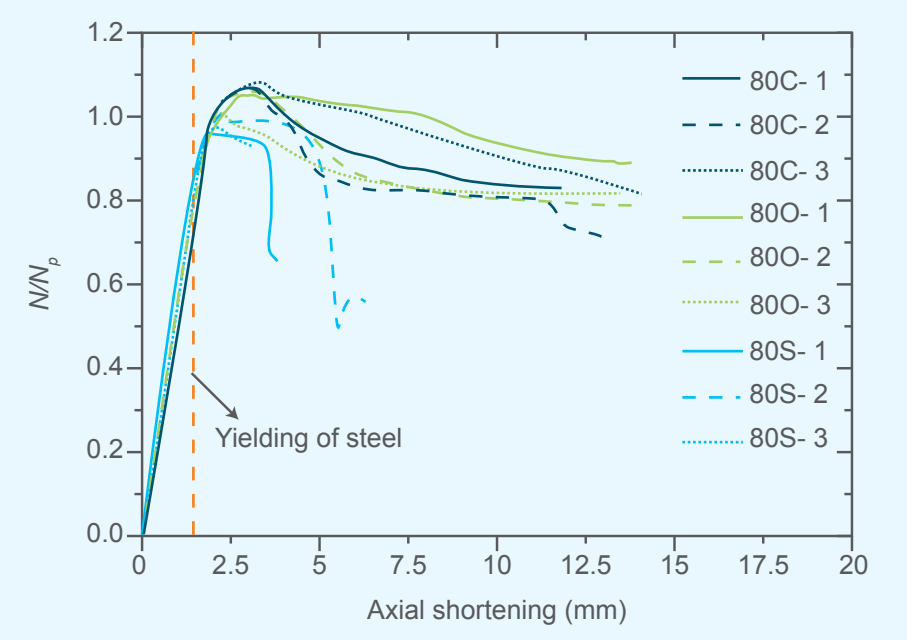

(c) C80/95

Figure 17 Normalized axial load-end shortening curves of CFST specimens

30C-1 50C-1 50O-1

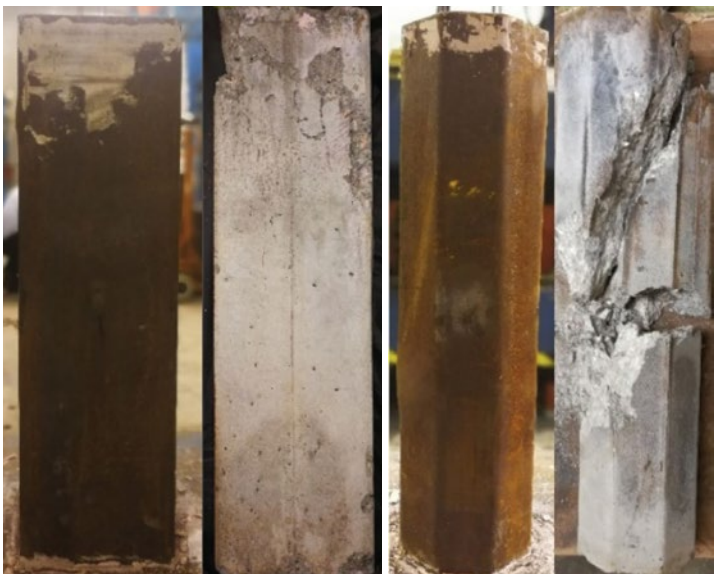

50S-1 80O-1

Figure 18 Failure mode of typical specimens

The test results show that under a high confinement ratio, the confinement effectiveness of octagonal CFST in terms of enhancement in axial resistance is not comparable to that in circular CFST; but is much better than that in square CFST. However, when the high strength concrete was used where the confinement ratio decreased, the difference in the enhancement in load capacity between circular and octagonal CFST becomes negligible.

The assessment of the test results indicates that the confinement effect on load capacity of octagonal CFST cannot be neglected and current design code for general cross-section shapes is not applicable. The design formula for load capacity could be developed by a basic superposition model with modification factors which is shown as follows:

$$N_d = a_s A_s f_y + (1 + a_c) A_c f'_c \tag{3}$$

where α_s is the reduction factor on steel tube as the axial stress of steel tube cannot reach the yield stress due to the biaxial stress condition, α_c is the enhancement factor to concrete core because of the effect of confinement, A_s and A_c are cross-sectional areas of the steel tube and the concrete core, respectively, f_y and f_c' are the yield strength of the steel tube and the concrete compressive cylinder strength. The steel tube in CFST is under the axial stress σ_a from the applied load and hoop stress σ_h from the dilation of concrete after the elastic stage. As the stress in concrete approaching its unconfined strength, the hoop strain increases rapidly and larger than that in steel tubes, then the steel tube starts to confine the concrete and the steel tube is under biaxial stress condition. To determine the reduction factor α_s, the hoop stress in steel tubes is critical. it is possible to obtain the reduction factor α_s in octagonal CFST by investigating the relationship between the hoop stress in the CFST with circular and octagonal section. A simple cross-section equilibrium is shown in Figure 19. Based on this equilibrium the hoop stress of octagonal could be derived as:

$$\sigma_{h,s} = \frac{f_1 (D_i - t)}{2t} \tag{4}$$

where $\sigma_{h,s}$ is the hoop stress of the steel tube, f_1 is the confining pressure and D_i is the inscribed diameter of the octagonal section.

$$D_i = (1+\sqrt{2})B \tag{5}$$

where B is the nominal width of the octagonal section including the corner radius. It was found that the hoop stress in steel tube of octagonal CFST is equal to that in CFST with the inscribed circular section. Based on this finding, the equivalent circular section with an inscribed diameter of D_i could be used to determine the reduction factor α_s where:

$$\alpha_{s,oct} = \alpha_{s,Di} \tag{6}$$

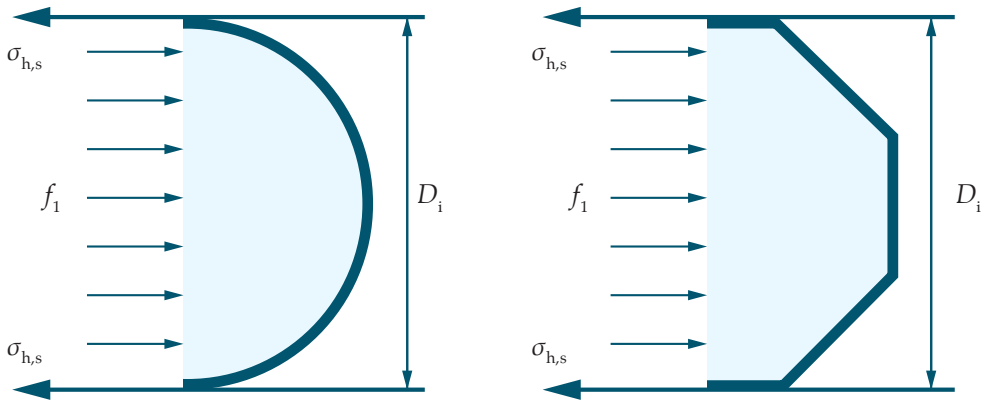

Figure 19 Force-equilibrium condition of circular and octagonal CFST

It is believed that under the same confinement ratio or material contribution ratio, the enhancement factor is only affected by the cross-sectional shapes of CFST and it is found that with the same tube thickness, the inscribed circular section shares the same confinement ratio with the original octagonal section. According to this assumption, it is possible to find a relationship between the enhancement factor α_c of octagonal section and that of its inscribed circular section which satisfies：

$$\alpha_{c,oct} = k\alpha_{c,Di} \tag{7}$$

where $\alpha_{c,Di}$ and $\alpha_{c,oct}$ are the enhancement factor of the inscribed circular section and the octagonal section respectively, k is the shape factor that reflect the confinement effectiveness. Figure 20 shows the relationship between the load capacity enhancement percentage in circular CFST $\alpha_{c,Di}$ and that in octagonal CFST, $\alpha_{c,oct}$. It could be found the relationship is approximately linear and the k value is about 0.73. Based on Eq. (6) and Eq. (7), the design formula for circular CFST in EN 1994-1-1, could be modified for the design of octagonal CFST as follows:

$$N_d = \eta_{a,Di} A_s f_y + A_c f'_c \left(1+0.73\eta_{c,Di} \frac{t}{D_i} \frac{f_y}{f_c}\right) \tag{8}$$

where $\eta_{a,Di}$ and $\eta_{c,Di}$ are the modification factors which could be calculated from Eq. (9) based on the equivalent inscribed circular section.

$$\eta_a = 0.25\left(3+2\bar{\lambda}\right) \le 1 \tag{9}$$

$$\eta_c = 4.9 - 18.5\bar{\lambda} + 17\bar{\lambda}^2 \ge 0$$

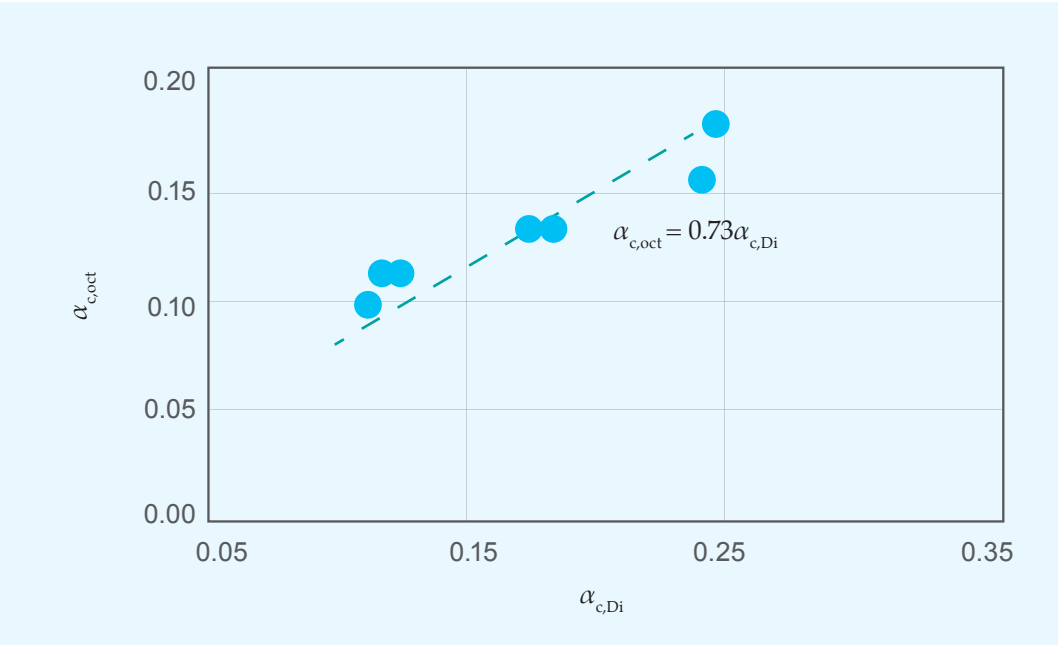

Figure 20 Relationship between the load capacity enhancement in circular and octagonal CFST

Figure 21 shows the assessment of the proposed design formula for octagonal CFST. It could be found that the modified design formula can provide a very close and conservative prediction on the load capacity of octagonal CFST comparing with existing design methods.

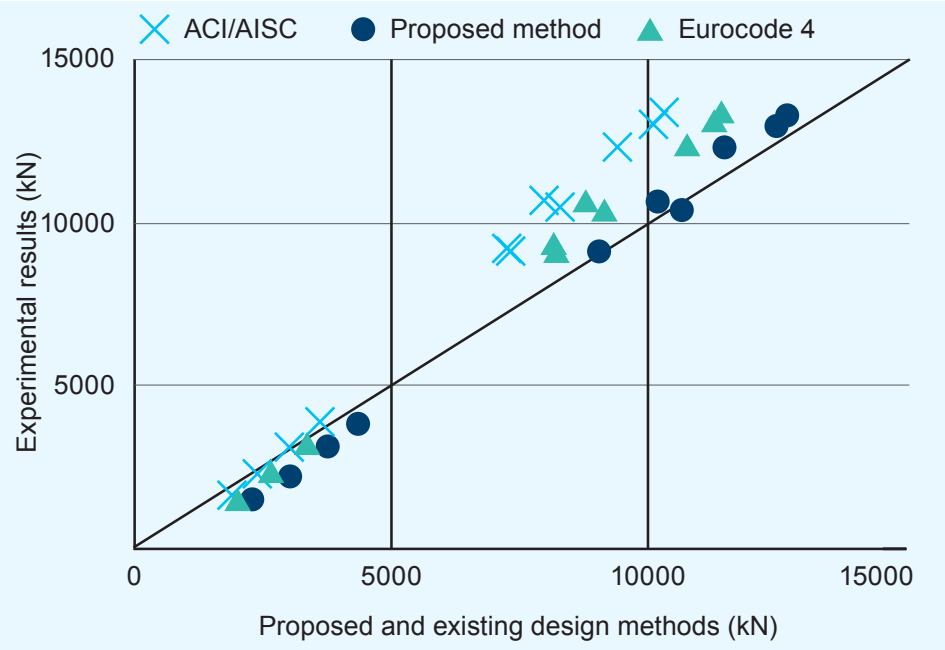

Figure 21 Assessment on the existing and proposed design methods for octagonal CFST

3.3 Octagonal CFST Beams and Beam-columns

Seventeen octagonal CFST beams and beam-columns infilled with different concrete grades as well as two hollow section counterparts were tested under cyclical lateral load with or without constant axial load. The test results of beam tests and beam-column tests are summarized in Table 3 and Table 4, respectively, while Figure 22 and Figure 23 present the moment and drift ratio curves of beam and beam-column tests.

Table 3 Summary of the test results and comparison with code provisions

Speci-men	Experimental results				EN 1994-1-1			AISC 360-16				
	$M_{1\%}$	M_{ue}	K_{ie}	E_h	$M_{pl,Rd}$	$M_{1\%}/M_{pl,Rd}$	K_{ic}	K_{ie}/K_{ic}	M_{AISC}	$M_{1\%}/M_{AISC}$	K_{ic}	K_{ie}/K_{ic}
	kNm	kNm	kNm·m	kNm	kNm	--	--	(kNm·m)	--	kNm	--	(kNm·m)
H-M	33.7	35.3	1867	-	33.4	1.011	1732	1.078	33.4	1.011	1732	1.078
H-C	33.3	37.5	1927	36.67	33.4	0.996	1732	1.113	33.4	0.996	1732	1.113
C30-M	38.6	47.6	2237	-	39.2	0.986	2170	1.031	38.7	0.997	2279	0.982
C30-C	39.7	44.5	2270	54.4	38.8	1.026	2170	1.046	38.4	1.036	2279	0.996
C60-M	39.9	48.5	2324	-	40.4	0.989	2281	1.019	39.8	1.002	2428	0.957
C60-C	40.2	45.1	2367	54.84	40.5	0.994	2281	1.038	39.9	1.008	2428	0.975
C90-M	40.1	50.6	2570	-	41.6	0.965	2349	1.094	40.9	0.980	2523	1.019
C90-C	41.0	45.4	2571	55.41	41.1	0.998	2349	1.095	40.5	1.014	2523	1.019
Mean						0.996		1.064		1.005		1.017
COV						0.018		0.033		0.016		0.052

Table 4 Summary of the test results and comparison with code provisions

Specimen	Experimental results					EN 1994-1-1				AISC 360-16			
	P_{ue}	M_{ue}	K_{ie}	E_h	$E_{h,4\%}$	$M_{pl,Rd}$	$M_{ue}/M_{pl,Rd}$	K_{ic}	K_{ie}/K_{ic}	M_{AISC}	M_{ue}/M_{AISC}	K_{ic}	K_{ie}/K_{ic}
	(kN)	(kNm)	(kNm·m)	(kNm)	(kNm)	(kNm)	-	(kNm·m)	-	(kNm)	-	(kNm·m)	-
S1	28.3	24.6	836	24.47	4.62	22.4	1.099	1122	0.745	22.2	1.107	1184	0.706
S2	22.6	25.0	1259	18.66	4.74	23.7	1.054	1128	1.116	23.5	1.063	1191	1.057
S3	21.3	22.3	1344	5.01	-	19.0	1.171	1127	1.193	18.9	1.181	1191	1.128
Mean							1.108		1.018		1.117		0.964
COV							0.054		0.235		0.059		0.235
S4	29.1	25.3	872	30.74	4.73	23.0	1.097	1198	0.728	22.8	1.108	1278	0.682
S5	27.3	27.7	1389	20.53	4.95	25.6	1.084	1203	1.155	25.3	1.097	1284	1.082
S6	23.6	26.7	1631	15.58	4.05	27.0	0.991	1200	1.359	26.5	1.008	1281	1.273
Mean							1.057		1.081		1.071		1.012
COV							0.055		0.298		0.051		0.298
S7	30.9	26.9	905	28.43	4.62	24.4	1.099	1309	0.691	24.0	1.117	1414	0.640
S8	26.4	29.5	1665	13.47	5.17	29.1	1.014	1332	1.250	28.4	1.038	1443	1.154
S9	22.6	28.8	2170	8.80	4.57	31.9	0.903	1320	1.644	31.1	0.926	1429	1.519
Mean							1.005		1.195		1.027		1.104
COV							0.098		0.401		0.093		0.400
Overall Mean							1.057		1.098		1.072		1.027
Overall COV							0.074		0.293		0.069		0.289

The effective flexural stiffness (K_i) of a composite section can be computed according to Eq. (10), where E and E_c are elastic moduli of the steel and concrete, respectively, I_s and I_c are moment of inertia of the steel tube and concrete, respectively, α is a correction factor to reduce the gross stiffness of the concrete which takes into account of the cracks in the concrete. The factor α takes different forms in different codes of practice, e.g. a constant of 0.6 in EN 1994-1-1 and a non-constant (see Eq. (11)) in AISC 360-16 (2016), where A_s and A_g are areas of steel tube and composite section.

$$K_i = EI_s + \alpha E_c I_c \tag{10}$$

$$\alpha = 0.45 + 3A_s / A_g \leq 0.9 \tag{11}$$

According to EN 1994-1-1, the cross-sectional resistance of CFST beam-columns can be obtained based on the axial force-bending moment interaction curve, as shown in Figure 24. As specified by EN 1994-1-1, the bending moment capacity can be calculated using the plastic stress distribution method assuming that the steel reaches its yield strength in both compression and tension and the concrete in compression reaches a stress of $\beta f_c'$, where f_c' is the concrete compressive cylinder strength and β is a shape factor for the concrete stress block. Generally, the shape factor is taken as 0.85 for reinforced concrete and composite members. However, according to the European code, for CFST members, this factor should be taken equal to unity. As illustrated in Figure 24, the nonlinear interaction curve, referring to the dashed line in Figure 24, can be calculated by varying the position of the neutral axis and establishing equilibrium of forces at the cross-section level. EN 1994-1-1 also allows for a simplified interaction curve using a polygonal diagram (see the solid line in Figure 24), which can be calculated using four points, referring to points A, B, C and D in Figure 24. Using the interaction curve, the ultimate bending resistance can be easily determined given a value of compressive axial load N, as expressed in Eq. (12).

$$\begin{cases} AC: \dfrac{N-N_{pm,Rd}}{N_{pl,Rd}-N_{pm,Rd}} + \dfrac{M_{pl,N,Rd}}{M_{pl,Rd}} = 1 \\ CD: \dfrac{N-0.5N_{pm,Rd}}{N_{pl,Rd}-0.5N_{pm,Rd}} + \dfrac{M_{pl,N,Rd}-M_{pl,Rd}}{M_{max,Rd}-M_{pl,Rd}} = 1 \\ BD: \dfrac{N}{0.5N_{pm,Rd}} + \dfrac{M_{pl,N,Rd}-M_{max,Rd}}{M_{p1,Rd}-M_{max,Rd}} = 1 \end{cases} \quad (12)$$

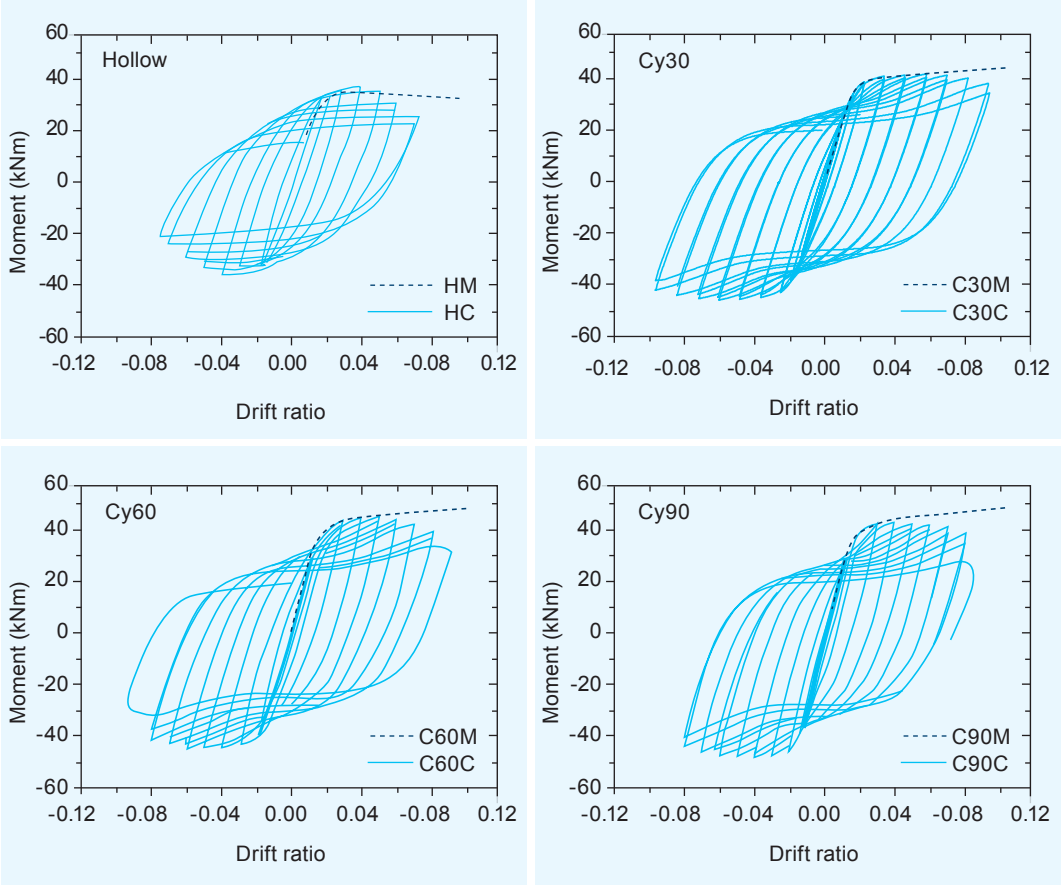

Figure 22 Moment and Drift ratio hysteretic curves of beam tests

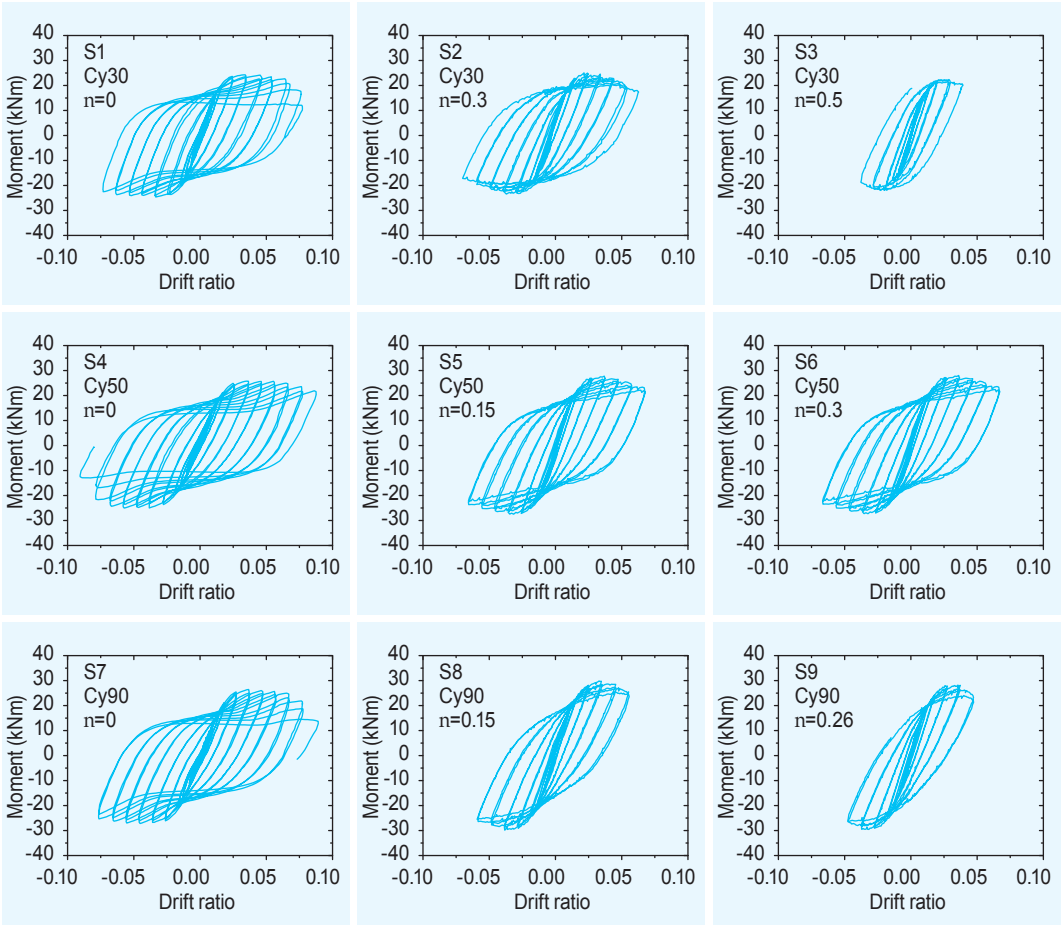

Figure 23 Moment and drift ratio hysteretic curves of beam-column tests

AISC 360-16 adopts different stress or strain distribution methods for the evaluation of the cross-section resistance for different cross-section classes, i.e. plastic stress distribution method for compact sections and strain compatibility method, elastic stress distribution method or effective stress-strain method for noncompact or slender sections respectively. Based on the assessment of the cross-section class of octagonal section using both circular and square/rectangular criteria, the octagonal section is classified as compact. Therefore, the plastic stress distribution method was adopted to evaluate the bending capacity of the octagonal CFSTs considered in this study. AISC 360-16 applies different values of the shape factor for circular and square/rectangular CFST beam-columns, i.e. 0.95 for circular sections and 0.85 for square/rectangular sections. As the American code does not prescribe any value for octagonal sections, in this study, a shape factor of 0.95 was assumed to evaluate the bending capacity according to AISC 360-16.

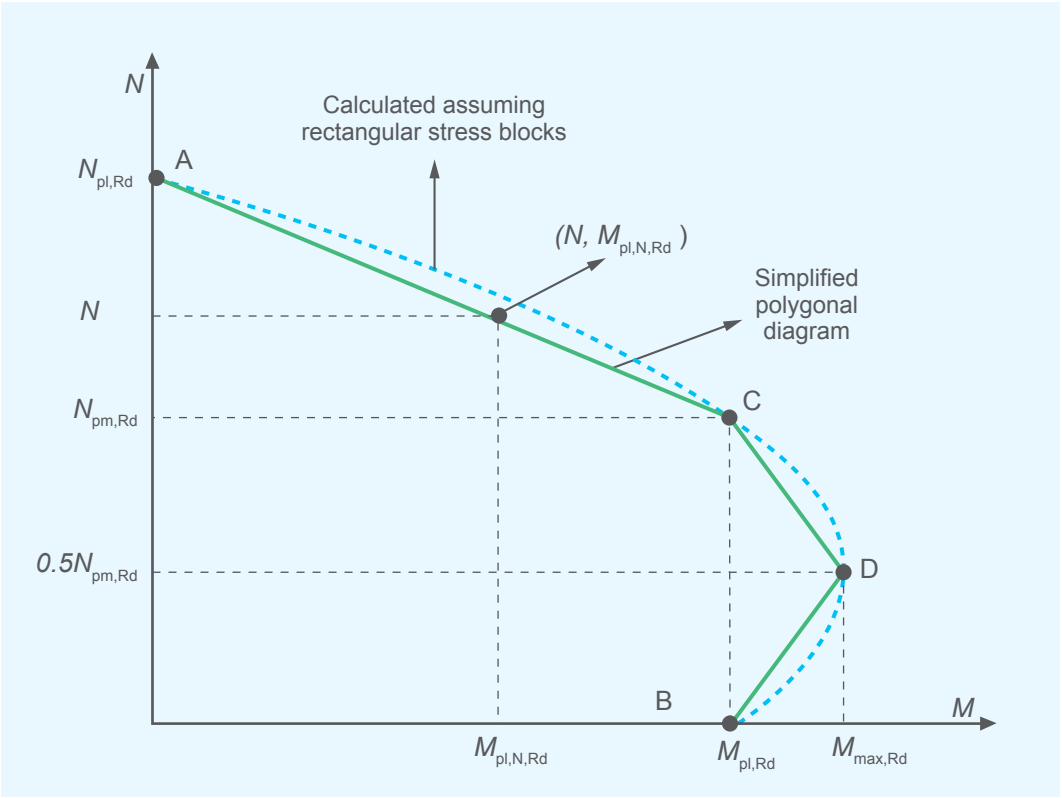

Figure 24 Interaction curve and corresponding stress distributions according to EN 1994-1-1

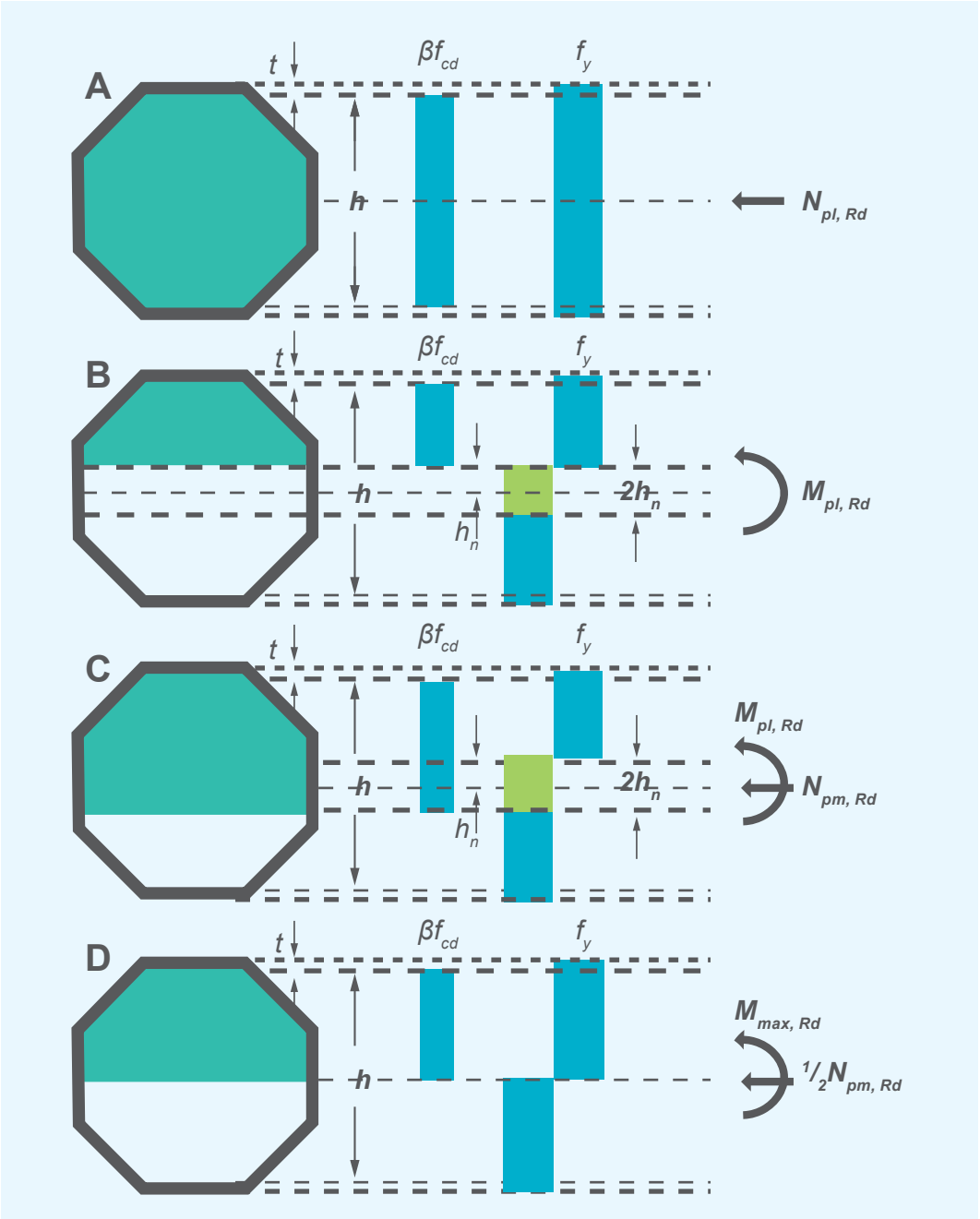

Figure 24 Interaction curve and corresponding stress distributions according to EN 1994-1-1

The effective flexural stiffness (K_i) of the octagonal CFST beams and beam-columns obtained from the test results were compared with those predicted from EN 1994-1-1 and AISC 360-16 to examine their accuracy in predicting the flexural stiffness of octagonal CFST beams and beam-columns. The comparisons of the effective flexural stiffness are summarized in Table 3 and Table 4, where K_{ie} is the flexural stiffness obtained from the test results and K_{ic} is the flexural stiffness predicted based on design codes. The results show that EN 1994-1-1 and AISC 360-16 predict the effective flexural stiffness well with mean values of K_{ie}/K_{ic} equal to 1.064 and 1.017, with the corresponding COVs of 0.033 and 0.052 for the beam tests. Regarding the beam-column tests, the results show that EN 1994-1-1 underestimates the effective flexural stiffness by nearly 10% with a mean K_{ie}/K_{ic} value 1.098 with the corresponding COV of 0.293, and AISC 360-16 predicts the effective flexural stiffness well with a mean value of K_{ie}/K_{ic} equal to 1.027 with the corresponding COV of 0.289, respectively.

The ultimate bending moments of the octagonal CFST beams and beam-columns obtained from the test results were compared with those predicted from EN 1994-1-1 and AISC 360-16 to examine the accuracy of the two codes in predicting the flexural strength of octagonal CFST beams and beam-columns. It should be stated that high strength concrete (Cy90) is not covered both in EN 1994-1-1 and AISC 360-16. However, in this study, the equations specified in these codes were still used to examine their accuracy for high strength concrete. Furthermore, to allow for a direct comparison, all partial safety factors were set to unity. The comparison results are listed in Table 3 and Table 4, indicating that EN 1994-1-1 predicts the ultimate bending moments quite well, if the resistance is obtained when the strain of extreme tension fibre reaches 0.01, with an overall mean value of $M_{1\%}/M_{pl,Rd}$ equal to 0.996 with the corresponding COV of 0.018, where $M_{1\%}$ is the ultimate moments obtained from test results and $M_{pl,Rd}$ is the ultimate moments predicted based on plastic stress block method. Since the shape factor (β) used in AISC 360-16 was 0.95, which is relatively smaller than unity which was used in EN 1994-1-1, the comparison result is slightly conservative with an overall mean value of $M_{1\%}/M_{AISC}$ equal to 1.005 with the corresponding COV of 0.016. The applicability of EN 1994-1-1 and AISC 360-16 to the design of octagonal CFST beams seems to be valid. As for octagonal beam-column tests, the comparison results indicate that EN 1994-1-1 predicts the ultimate bending moments quite well with an overall mean value of $M_{ue}/M_{pl,Rd}$ equal to 1.057 with the corresponding COV of 0.074, where M_{ue} is the ultimate moments obtained from test results and $M_{pl,Rd}$ is the ultimate moments predicted based on plastic stress block method.

Since the shape factor (β) used in AISC 360-16 was 0.95, which is relatively smaller than unity which was used in EN 1994-1-1, the comparison result is slightly conservative with an overall mean value of M_{ue}/M_{AISC} equal to 1.072 with the corresponding COV of 0.069. The applicability of EN 1994-1-1 and AISC 360-16 to the design of octagonal CFST beam-columns seems to be valid and on the conservative side with underestimations of 5.7% and 7.2% of the flexural capacity, respectively. Comparing the specimens infilled with different concrete grades, the predictions using both design codes seem to be more conservative for normal strength concrete than for high strength concrete, as the mean values of $M_{ue}/M_{pl,Rd}$ for the specimens infilled with Cy30, Cy50 and Cy90 concrete are 1.108, 1.057 and 1.005 using EN 1994-1-1, respectively, and 1.117, 1.071 and 1.027 using AISC 360-16.

In summary, it is viable to extend the current design rules prescribed in EN 1994-1-1 and AISC 360-16 to the design of octagonal CFST beams and beam-columns with slight underestimate of the capacity. For conservativeness, a reduction factor may need to be incorporated for the design of octagonal CFST members made with high strength concrete. EN 1994-1-1 and AISC 360-16 predict the effective flexural stiffness of CFST beams and beam-columns quite well with acceptable effectiveness and conservatism.

3.4 Analytical Hysteretic Model

In this study, the hysteretic model for octagonal CFST beams and beam-columns was proposed based on the test results by modifying the hysteretic models developed in Han *et al.* (2003) and Han and Yang (2005). A schematic view of the hysteretic model is shown in Figure 25. The hysteretic models could be used in frame analyses as zero length rotational springs, as illustrated in Figure 26.

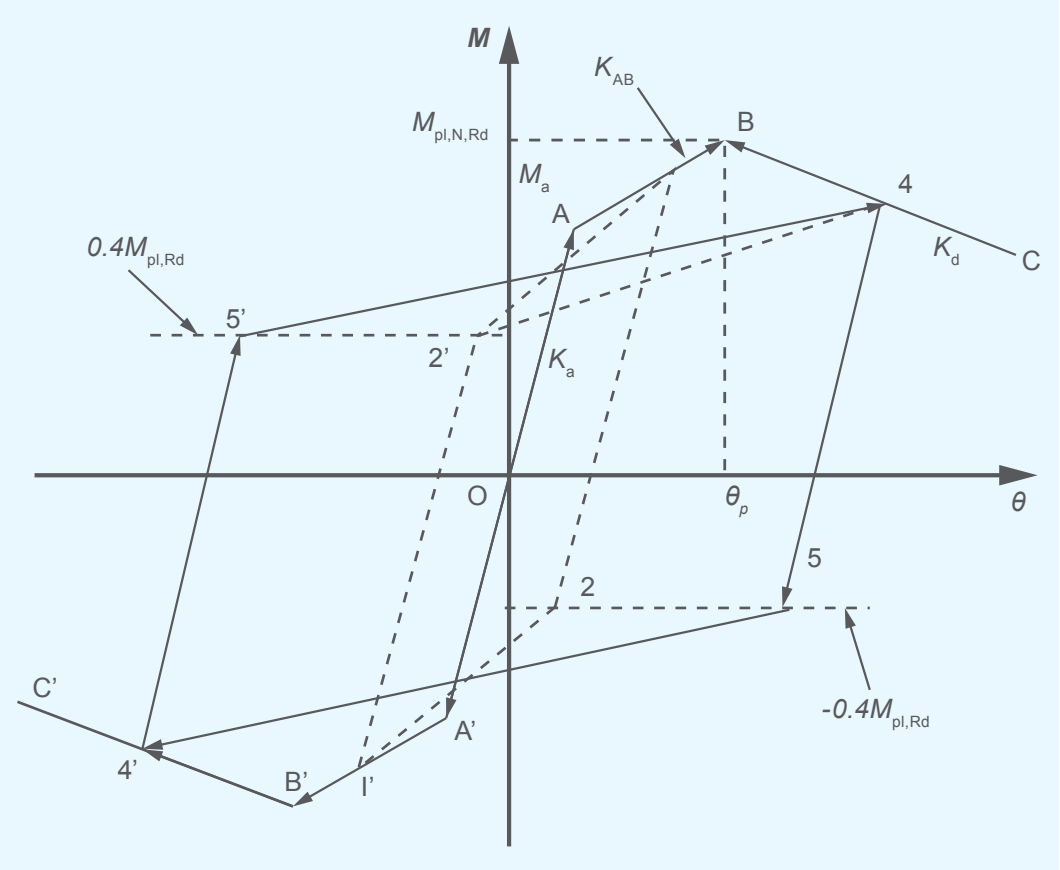

Figure 25 A schematic view of the hysteretic model

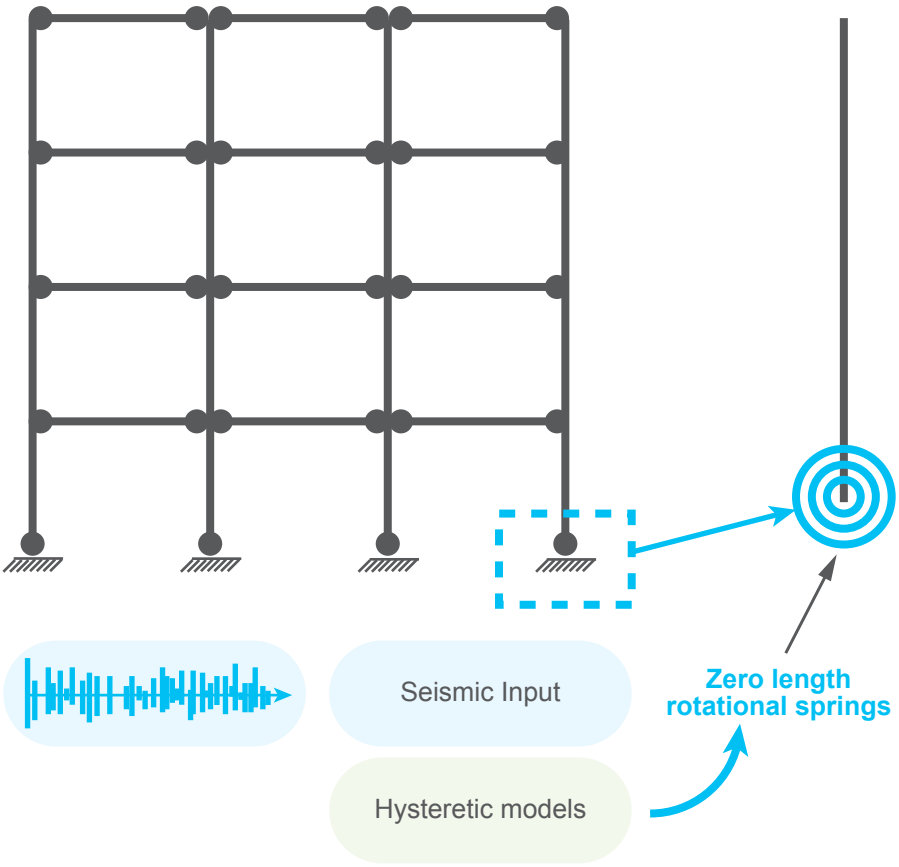

Figure 26 Seismic frame analyses using rotational springs

The hysteretic model (*M*-*θ* behaviour) for octagonal CFST beams and beam-columns is as follows:

1. Ultimate moment capacity ($M_{pl,N,Rd}$) corresponding to point B in Figure 25 under a certain axial load, *N*, could be determined according to the axial force-bending moment interaction curve (expressed in Eq. (12)), as shown in Figure 24, or directly observed from test results.

2. Stiffness in the elastic stage (K_a) up to yield moment (M_a) corresponding to point A in Figure 25 is given by Eq. (13) based on Han *et al.* (2003) and Han and Yang (2005).

$$K_a = \frac{24K_e}{L^3} \cdot \mathrm{L}^2 \tag{13}$$

where L is the effective buckling length of column in the plane of bending, K_e could be given by Eq. (14) based on EN 1994-1-1.

$$K_e = E_s I_s + 0.6 E_e I_e \tag{14}$$

where E_s, E_c, I_s, and I_s are elastic moduli of steel and concrete, moment of inertia for hollow steel tube and the concrete core, respectively. The moment corresponding to Point A (M_a) in Figure 25 could be taken as $0.8M_{pl,N,Rd}$ based on the experimental observations.

3. Based on the experimental observations, stiffness in the inelastic stage (K_{AB}) up to the ultimate moment capacity ($M_{pl,N,Rd}$) could be determined by $0.2K_a$, while the stiffness in the descending stage (K_d) could be given by Eq. (15). n is axial load ratio.

$$K_d = -(0.02+0.2n)K_a \tag{15}$$

The moments at point 2 and point 2', point 5 and point 5' (as shown in Figure 24) are given by $-0.4M_{pl,N,Rd}$ and $0.4M_{pl,N,Rd}$ respectively, based on the experimental observations.

To assess the accuracy of the analytical hysteretic model on predicting the cyclic behaviour of octagonal CFST beams and beam-columns, the results of the analytical model were compared with the beam and beam-column test results.

CFST Beam Tests

The comparisons of the hysteretic curves obtained from the analytical hysteretic model with beam tests are presented in Figures 27, while Table 5 summarises the comparison results of the ultimate bending moments, initial effective stiffness and the dissipated energies, indicating that the analytical hysteretic model predicts the hysteretic behaviour with acceptable accuracy with mean values of M_{ue}/M_{um}, K_{ie}/K_{im} and E_{he}/E_{hm} equal to 1.122, 1.059 and 1.011, respectively, and with the corresponding COVs of 0.020, 0.029 and 0.007, respectively, where M_{ue} is the ultimate moments obtained from test results, M_{um} is the ultimate moments predicted from the analytical model, K_{ie} is the flexural stiffness obtained from the test results, K_{im} is the predicted flexural stiffness, E_{he} is the cumulative hysteresis dissipated energy from test results, and E_{hm} is the cumulative hysteresis dissipated energy predicted from the analytical model.

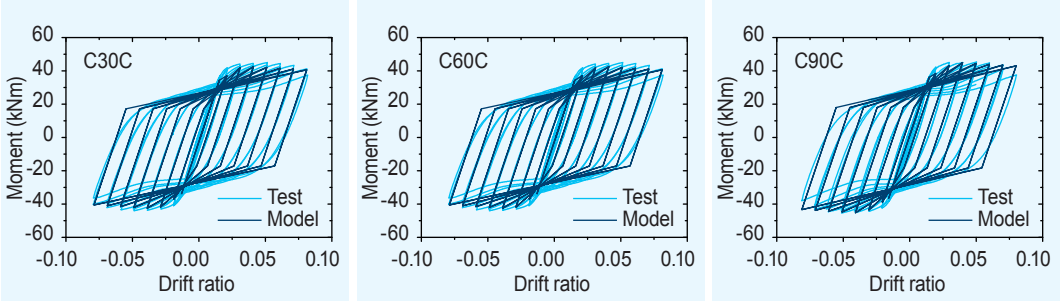

Figure 27 The comparisons of the analytical hysteretic model with beam tests

Table 5 The comparisons of the analytical hysteretic model with beam tests

Speci-men	Experimental results			Model					
	M_{ue}	K_{ie}	E_{he}	M_{um}	M_{ue}/M_{um}	K_{im}	K_{ie}/K_{im}	E_{hm}	E_{he}/E_{hm}
	(kNm)	(kNm·m)	(kNm)	(kNm)	-	(kNm·m)	-	(kNm)	
C30C	44.54	2270	54.4	38.79	1.148	2170	1.046	53.36	1.019
C60C	45.05	2367	54.84	40.47	1.113	2281	1.038	54.54	1.006
C90C	45.43	2571	55.41	41.09	1.106	2349	1.095	54.92	1.009
Mean					1.122		1.059		1.011
COV					0.020		0.029		0.007

CFST Beam-column Tests

The comparisons of the hysteretic curves obtained from the analytical hysteretic model with beam-columns are presented in Figures 28, while Table 6 summarises the comparison results of the ultimate bending moments, initial effective stiffness and the dissipated energies, indicating that the analytical hysteretic model predicts the hysteretic behaviour quite well with mean values of M_{ue}/M_{um}, K_{ie}/K_{im} and E_{he}/E_{hm} equal to 1.057, 1.098 and 0.965, respectively, and with the corresponding COVs of 0.074, 0.293 and 0.073, respectively, where M_{ue} is the ultimate moments obtained from test results, M_{um} is the ultimate moments predicted from the analytical model, K_{ie} is the flexural stiffness obtained from the test results, K_{im} is the predicted flexural stiffness, E_{he} is the cumulative hysteresis dissipated energy from test results, and E_{hm} is the cumulative hysteresis dissipated energy predicted from the analytical model.

Table 6 The comparisons of the hysteretic model with beam-column tests

Speci-men	Experimental results			Model					
	M_{ue}	K_{ie}	E_h	M_{um}	M_{ue}/M_{um}	K_{im}	K_{ie}/K_{im}	E_{hm}	E_{he}/E_{hm}
	(kNm)	(kNm·m)	(kNm)	(kNm)	-	(kNm·m)	-	(kNm)	
S1	24.61	836	24.47	22.40	1.099	1122	0.745	26.68	0.917
S2	24.97	1259	18.66	23.70	1.054	1128	1.116	20.61	0.905
S3	22.28	1344	5.01	19.02	1.171	1127	1.193	5.65	0.887
S4	25.27	872	30.74	23.04	1.097	1198	0.728	28.50	1.079
S5	27.72	1389	20.53	25.57	1.084	1203	1.155	21.48	0.956
S6	26.71	1631	15.58	26.96	0.991	1200	1.359	14.72	1.058
S7	26.86	905	28.43	24.44	1.099	1309	0.691	29.32	0.970
S8	29.49	1665	13.47	29.07	1.014	1332	1.250	14.91	0.903
S9	28.84	2170	8.80	31.94	0.903	1320	1.644	8.70	1.011
Mean					1.057		1.098		0.965
COV					0.074		0.293		0.073

The comparisons with a good agreement between the analytical model and the test results indicate that the analytical hysteretic model could predict the cyclic behaviour of the octagonal CFST beams and beam-columns with acceptable effectiveness and conservatism.

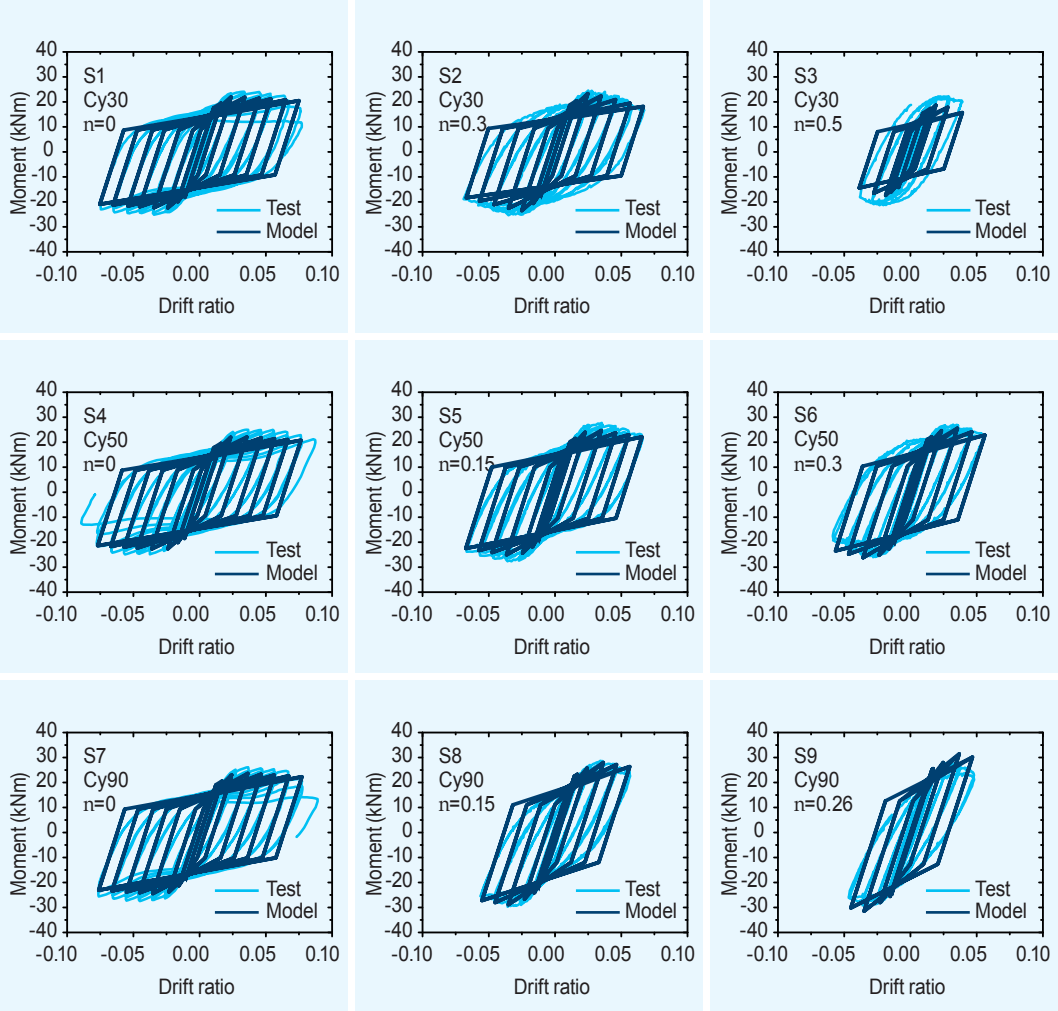

Figure 28 The comparisons of the hysteretic model with beam-column tests

4 RECOMMENDATIONS

Based on the experimental and analytical results from this project, a series of recommendations regarding the octagonal hollow and concrete-filled steel tubular columns have been proposed.

4.1 Cross-section Slenderness Limit for Octagonal Hollow Sections

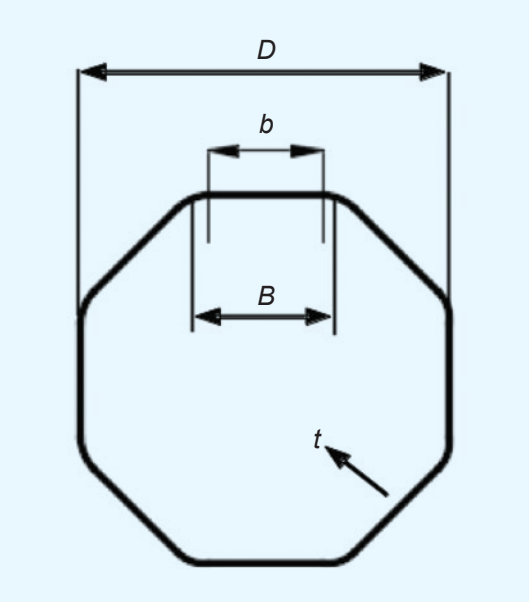

A new slenderness limit for plate buckling in octagonal cross-section was proposed by the regression analysis on the experimental and FE results as shown in Figure 15.

$$b / t \leq 29.8 \sqrt{(235 / fy)}$$

An alternative way for the section classification of octagonal cross-section could use the slenderness parameter in circular cross-section which is related to the *D/t* ratio. The equivalent circle with the same perimeter of the octagonal cross-section measured at the mid-thickness level, D_p, is suggested as the equivalent diameter with a circular section sharing the same cross-sectional area with the original octagonal cross-section. It is concluded that an equivalent circle approach could be adopted for the section classification of octagonal cross-sections based on EN1993-1-1, as shown in Figure 16.

$$D_p / t \leq 90(235 / f_y)$$

4.2 Axial Capacity Equations Considering Confinement Effect

Based on test observations, the design formula for circular CFST in EN 1994-1-1, could be modified for the design of octagonal CFST as follows:

$$N_d = \eta_{a,Di} A_s f_y + A_c f'_c \left(1+0.73\eta_{c,Di} \frac{t}{D_i} \frac{f_y}{f_c}\right)$$

$$\eta_a = 0.25\left(3+2\bar{\lambda}\right) \leq 1$$

$$\eta_c = 4.9-18.5\bar{\lambda}+17\bar{\lambda}^2 \geq 0$$

where $\eta_{a,Di}$ and $\eta_{c,Di}$ are the modification factors which could be calculated from the equations below based on the equivalent inscribed circular section.

4.3 Octagonal CFST Beams and Beam-columns

It is viable to extend the current design rules prescribed in EN 1994-1-1 to the design of octagonal CFST beams and beam-columns with slight underestimation of the capacity. For conservativeness, a reduction factor may be needed to be incorporated for the design of octagonal CFST members made with high strength concrete.

4.4 Analytical Hysteretic Model

The hysteretic model (*M*-*θ* behaviour) for octagonal CFST beams and beam-columns is as follows:

1. Ultimate moment capacity ($M_{pl,N,Rd}$) corresponding to point B in Figure 25 under a certain axial load, *N*, could be determined according to the axial force-bending moment interaction curve (expressed in Eq. (12)), as shown in Figure 24, or directly observed from test results.

2. Stiffness in the elastic stage (K_a) up to yield moment (M_a) corresponding to point A in Figure 25 is given by the equation.

$$K_a = \frac{24K_e}{L^3} \cdot \mathrm{L}^2$$

where L is the effective buckling length of column in the plane of bending, K_e could be given by the equation below based on EN 1994-1-1.

$$K_e = E_s I_s + 0.6 E_c I_c$$

where E_s, E_c, I_s, and I_s are elastic moduli of steel and concrete, moment of inertia for hollow steel tube and the concrete core, respectively. The moment corresponding to Point A (M_a) in Figure 25 could be taken as $0.8M_{pl,N,Rd}$ based on the experimental observations.

3. Based on the experimental observations, stiffness in the inelastic stage (K_{AB}) up to the ultimate moment capacity ($M_{pl,N,Rd}$) could be determined by $0.2K_a$, while the stiffness in the descending stage (K_d) could be given by the equation below. n is axial load ratio.

$$K_d = -(0.02+0.2n)\, K_a$$

The moments at point 2 and point 2', point 5 and point 5' (as shown in Figure 7.2) are given by $-0.4M_{pl,N,Rd}$ and $0.4M_{pl,N,Rd}$ respectively, based on the experimental observations.

5 REFERENCES

ABAQUS /Standard. (2013). Version 6.13-1. USA: K. a. S. Hibbit.

AISC. (2016). ANSI/AISC 360-16, Specification for structural steel buildings. American Institute of Steel Construction (AISC), Chicago (IL).

ASCE. (2011). ASCE/SEI 48-11, Design of steel transmission pole structures. American Society of Civil Engineers (ASCE); Reston, Virginia.

CEN. (2004). EN 1992-1-1, Eurocode 2 – Design of concrete structures–Part 1-1: General rules and rules for buildings. CEN (European Committee for Standardization), Brussels.

CEN. (2004). EN 1994-1-1, Eurocode 4 – Design of steel structures – Part 1.1: General rules and rules for buildings. CEN (European Committee for Standardization), Brussels.

CEN. (2004). EN 1998-1, Eurocode 8 – Design of structures for earthquake resistance–Part 1: General rules– Seismic actions and rules for buildings. CEN (European Committee for Standardization), Brussels.

CEN. (2005). EN 1993-1-1, Eurocode 3 – Design of concrete structures–Part 1-1: General rules and rules for buildings. CEN (European Committee for Standardization), Brussels.

Chan T.M., Gardner L., Law K.H. (2010). Structural design of elliptical hollow sections: a review. Structures and Buildings, Proceedings of Institution of Civil Engineers, 16: 391–402.

CoP Concrete (2013). Code of practice for the structural use of concrete 2013. Buildings Department, Hong Kong.

CoP Steel (2011). Code of practice for structural use of steel 2011. Buildings Department, Hong Kong.

Han L.H., Yang Y.F., Tao Z. (2003). Concrete-filled thin-walled steel SHS and RHS beam-columns subjected to cyclic loading. Thin-Walled Structures. 41(9): 801-833.

Han L.H., Yang Y.F. (2005). Cyclic performance of concrete-filled steel CHS columns under flexural loading. Journal of Constructional Steel Research. 61(4): 423-452.

Legislative Council (2014). Consultation on introduction of seismic-resistant building design standards in Hong Kong. CB (1) 1110/13-14(01), Panel on Development, Legislative Council, The Hong Kong Special Administrative Region.

Sheehan T., Chan T.M. (2014). Cyclic response of hollow and concrete-filled circular hollow section braces. Proceedings of Institution of Civil Engineers – Structures and buildings. 167(SB3), 140-152.

Members of CIC Task Force on Research

Mr. Jimmy TSE
Prof. Christopher LEUNG
Ir Joseph MAK
Prof. James PONG
Prof. Sze-chun WONG
Ir Chi-chiu CHAN
Ir Tommy NG
Mr. Shu-jie PAN

Research Team

Project Coordinator

Dr Tak-Ming CHAN

Deputy Project Coordinator

Prof. Siu-Lai CHAN

Research Personnel

Mr Jiongyi ZHU
Mr Junbo CHEN

建造業議會
Construction Industry Council

Address 地址：38/F, COS Centre, 56 Tsun Yip Street, Kwun Tong, Kowloon
九龍觀塘駿業街56號中海日升中心38樓

Tel 電話：(852) 2100 9000

Fax 傳真：(852) 2100 9090

Email 電郵：enquiry@cic.hk

Website 網址：www.cic.hk

cic_hk

HKCIC

Construction Industry Council

CICHK

HKCIC

Construction Industry Council Hong Kong

2018

CIC Research Report No. CICRS_027